

Two-Stage Robust Edge Service Placement and Sizing under Demand Uncertainty

Duong Tung Nguyen, Hieu Trung Nguyen, Ni Trieu, and Vijay K. Bhargava

Abstract—Edge computing has emerged as a key technology to reduce network traffic, improve user experience, and enable various Internet of Things applications. From the perspective of a service provider (SP), how to jointly optimize the service placement, sizing, and workload allocation decisions is an important and challenging problem, which becomes even more complicated when considering demand uncertainty. To this end, we propose a novel two-stage adaptive robust optimization framework to help the SP optimally determine the locations for installing their service (i.e., placement) and the amount of computing resource to purchase from each location (i.e., sizing). The service placement and sizing solution of the proposed model can hedge against any possible realization within the uncertainty set of traffic demand. Given the first-stage robust solution, the optimal resource and workload allocation decisions are computed in the second-stage after the uncertainty is revealed. To solve the two-stage model, in this paper, we present an iterative solution by employing the column-and-constraint generation method that decomposes the underlying problem into a master problem and a max-min subproblem associated with the second stage. Extensive numerical results are shown to illustrate the effectiveness of the proposed two-stage robust optimization model.

Index Terms—Edge computing, service placement, workload allocation, adaptive robust optimization, demand uncertainty.

I. INTRODUCTION

Edge computing (EC) has been proposed to augment the traditional cloud computing model to meet the soaring traffic demand and accommodate diverse requirements of various services and systems in future networks, such as embedded artificial intelligence (AI), 5G wireless systems, virtual/augmented reality (VR/AR), and tactile Internet [1], [2]. By distributing storage, computing, control, and networking resources closer to the network edge, EC offers remarkable advantages and capabilities, including local data processing and analytics, localized services, edge caching, edge resource pooling and sharing, and improved privacy and security [3], [4]. Also, EC is a key enabler for ultra-reliable low-latency applications.

To enhance user experience and reduce bandwidth usage, content/application/service providers (e.g., AR/VR companies, Google, Netflix, Facebook, Uber, Apple, and other OTT providers) can proactively install their applications, especially latency-sensitive and/or data-intensive ones such as AR/VR, cloud gaming, and video analytics, onto selected edge nodes (EN) in proximity of their users. Therefore, in addition to local execution on end-devices and remote processing in public clouds or their private data centers (DC), the SPs can offload their tasks to edge servers. Besides SPs, virtual network operators, vertical industries, enterprises, and other third parties (e.g., schools, hospitals, malls, sensor networks) can also outsource their data and computation to EC systems.

Fig. 1 depicts the new network architecture with an EC layer lying between the cloud and the aggregation layer. In

particular, the aggregation layer consists of numerous Points of Aggregation (POA), such as base stations (BS) and network routers/switches, which aggregate data and requests from users, things, and sensors. In practice, various sources (e.g., Telco edge clouds, telecom central offices, servers at BSs, PCs in research labs, micro DCs in campus buildings, malls, and enterprises) can act as ENs [1]–[4]. Indeed, an EN can be co-located with a POA. For example, edge servers can be placed in cell sites or deployed near routers in enterprise DCs.



Fig. 1: Edge Network Architecture

Typically, a service request first arrives at a POA, then it will be routed to an EN or the remote cloud for processing. For instance, with EC, when a user submits a Google Maps request or an Uber ride request, the request can now be handled by an EN instead of going all the way to the remote servers of Google or Uber. Clearly, EC not only can help the SP drastically improve the service quality but also significantly lower network bandwidth consumption.

Despite tremendous potential, EC is still in its infancy stage and many interesting open problems remain to be solved. In this work, we focus on the optimal edge service placement and workload allocation from the perspective of a SP (e.g., AR/VR, Pokémon Go, real-time translation, Uber, Apple Siri, Amazon Alexa, Google Assistant, Google Maps). Specifically, the SP needs to serve a large number of users/subscribers located in different areas. The goal of the provider is to minimize the total operating cost while maximizing the service quality. Here, we measure the quality of service (QoS) in terms of network delay.

In order to reduce the delay between the users and computing nodes, the SP can provision the service on various distributed ENs. Then, each user request can be processed by its closest ENs, which have the service installed. It is easy to see that placing the service on more ENs can lower the overall delay, but it also increases the SP's cost. Specifically, when the service is available on more ENs, the network delay decreases because requests in each service area can be routed to the ENs closer to them. On the other hand, the service placement cost increases when the service is installed on more ENs. Hence,

there is an inherent trade-off between the operating cost of the SP and the overall network delay of the requests.

Furthermore, unlike the traditional cloud with virtually infinite capacity, ENs often have limited computational power [1]–[3]. Additionally, in contrast to a small number of cloud DCs, there are numerous heterogeneous distributed ENs coming with different sizes and configurations. The resource prices of the ENs can also be different due to various factors such as different hardware specifications, electricity prices, location, reliability, reputation, and ownership. Thus, some ENs close to the users may not be chosen because of their higher prices. As a result, selecting suitable ENs for service placement is a challenging task due to the heterogeneity of the ENs.

Besides the placement decisions, the SP also needs to decide the amount of resource to buy from each selected EN. Given the service placement and sizing decisions, the provider will then decide how to allocate the traffic demand in different areas to different ENs to minimize the overall network delay. To this end, when the traffic demand is known, we formulate the joint service placement, resource sizing, and workload allocation problem as a mixed integer linear program (MILP), which can be solved efficiently by leveraging the state-of-the-art MILP solvers. The formulated problem aims to minimize the weighted sum of the operating cost of the SP and the total network delay of the user requests, while taking into account practical system design criteria such as resource capacity limits, budget constraint, and delay preference.

This problem becomes more sophisticated when considering the demand uncertainty. For example, in practice, the SP normally solves the deterministic MILP formulation using the forecast demand to find the optimal resource provisioning solution (i.e., placement and sizing). However, since the actual demand is unknown to the SP at the time of making decision, over-provisioning or under-provisioning may occur frequently, which is undesirable. Specifically, if the procured resources are excessive to serve the actual traffic demand most of the time, it leads to over-provisioning and unnecessarily high provisioning cost. On the other hand, if the procured resources are not sufficient to serve the actual demand most of the time, it leads to under-provisioning and may severely affect the quality of service (e.g., high latency, dropping requests).

A popular technique to deal with uncertainty is stochastic optimization, which has been successfully applied to many engineering problems, including cloud resource provisioning [5]–[7]. However, the stochastic optimization approach requires to know the probability distribution of uncertain data, which is often difficult to obtain. Also, to ensure the solution quality, in stochastic programming, we need to generate a large set of scenarios based on this probability distribution and associate each scenario with a certain probability. Hence, even if the distribution is known, the stochastic model can still be computationally prohibitive, and even intractable.

Recently, robust optimization (RO) [8] has emerged as an alternative methodology to handle data uncertainty. Since the RO approach does not require knowledge of probability distribution of the uncertainty, it can avoid some of the difficulties arising from the stochastic programming approach. Indeed, RO has also been applied in the context of cloud resource management [9]–[11]. Unlike stochastic programming where

uncertainty is captured by a large number of scenarios, uncertainty in RO is described by parametric sets, called uncertainty sets. Since uncertainty sets can be constructed simply by using information such as lower bounds and upper bounds of uncertain parameters (i.e., random variables), it is much easier to derive than exact probability distributions.

The goal of RO is to find a robust solution that not only optimizes system performance but can also hedge against any perturbation in the input data within the uncertainty sets. Thus, the solution to a RO model tends to be conservative. However, the conservativeness of robust solutions can be controlled by adjusting the uncertainty sets whose forms significantly affect the tractability and computational complexity of a robust model [8]. Furthermore, while a larger uncertainty set strengthens the robustness of a solution, it also increases the conservativeness. In practice, RO models usually scale well with the increasing dimension of data and are computationally tractable for large-scale systems. Additionally, uncertainty sets are often constructed based on the desired level of robustness, historical data and experience of the decision maker.

In RO models, all decisions are made before the uncertainty is revealed, which can be overly conservative. To tackle this issue, adaptive robust optimization (ARO) [12], also known as two-stage RO [13], has recently been introduced, where the second-stage problem models recourse decisions after observing the first-stage decisions and the realization of the uncertainty. The first-stage decisions are often referred as “*here-and-now*” decisions that cannot be adjusted after the uncertainty is disclosed, while the second-stage decisions are known as “*wait-and-see*” decisions that can be adjusted and adapted to the actual realization of uncertain data. Thus, ARO is still robust while less conservative than RO.

In this paper, to address the challenge caused by the demand uncertainty, we propose a novel two-stage RO model to help the SP identify optimal ENs for placing the service and optimal amount of resource procured from each node before knowing the actual demand. The service placement and sizing are the first-stage decisions that are robust against any realization of traffic demand within a predefined uncertainty set. Given the first-stage solution, the optimal workload allocation decision is made in the second-stage after the uncertainty is disclosed.

The rationale behind this design is that service placement and sizing typically happen at a larger time scale (e.g., in the order of hours or days) to ensure system stability [14] while the workload allocation decisions can be adjusted in a shorter time scale (e.g., every few minutes) based on the actual demand. Furthermore, in practice, the SP may not be able to change the resource procurement decision frequently in short time scale. Hence, the two-stage RO approach is a reasonable modeling choice for our problem. Note that the first-stage decision is robust against all scenarios, including the worst-case one, contained in the uncertainty set. If the realized demand is not the worst case, the workload allocation can be updated based on the actual demand in the operation stage.

To the best of our knowledge, this is the first two-stage robust model for the edge service placement and sizing problem. Our main contributions are summarized below:

- We first introduce a deterministic MILP model for joint edge service placement, resource procurement, and work-

load allocation, which is then extended to a new two-stage RO model to deal with demand uncertainty. In particular, the first-stage decision variables include service placement and resource sizing, while resource allocation and request scheduling are the second-stage decisions.

- The formulated model is a trilevel optimization problem that is decomposed into a master problem and a max-min subproblem. The bilevel subproblem is reformulated into a single-level problem with complementary constraints, which is then transformed into an MILP. We develop an iterative algorithm based on the column and constraint generation (CCG) method [13] to solve the problem in a master-subproblem framework, which is guaranteed to converge in a finite, typically small, number of iterations.
- Finally, extensive numerical results are presented to demonstrate the efficacy of the proposed ARO model compared to the deterministic and RO models. We also perform sensitivity analysis to evaluate the impacts of different system parameters on the optimal solution.

The rest of the paper is organized as follows. In Section II, we describe the system model. In Section III, we first formulate the deterministic optimization model, which is then extended to a static robust model and an adaptive robust model. The CCG-based iterative solution approach is introduced in Section IV. Simulation results are shown in Section V followed by discussion of related work in Section VI. Finally, we present conclusions and future research directions in Section VII.

II. SYSTEM MODEL

TABLE I: NOTATIONS

Notation	Meaning
EN, AP	Edge Node, Access Point
\mathcal{M}, M	Set and number of APs
\mathcal{N}, N	Set and number of ENs
i, j	AP index and EN index
C_j	Resource capacity of EN j available for purchase
p_0	Price of one computing unit at the cloud
p_j	Price of one computing unit at EN j
f_j	Service placement cost at EN j
s_j	Storage cost at EN j
D^m	Delay threshold
$d_{i,0}$	Network delay between AP i and the cloud
$d_{i,j}$	Network delay between AP i and EN j
B	Budget of the service provider
β	Weighting factor, delay cost
w	Computing resource demand of one request
λ_i^f	Forecast traffic demand at AP i
λ_i	Actual traffic demand at AP i
C^d	Total network delay cost
C^c	Cloud resource procurement cost
C_j^p	Service placement cost at EN j
C_j^e	Edge resource procurement cost at EN j
C_j^s	Storage cost at EN j
$x_{i,0}$	Workload at AP i assigned to the cloud
$x_{i,j}$	Workload at AP i assigned to EN j
y_0	Amount of computing resource purchased at the cloud
y_j	Amount of computing resource purchased at EN j
z_j^0	$\{0, 1\}$, 1 if the service is placed at EN j at the beginning
z_j	Binary variable, 1 if the service is placed at EN j
Γ	Uncertainty budget
\mathcal{D}	Demand uncertainty set

In this paper, we study the service placement and sizing from the perspective of a SP (e.g., Google Maps, AR/VR).

The SP has subscribers located in different areas, where user requests in each area are aggregated at an access point (AP). Without EC, the requests are typically sent to remote servers for processing. However, with EC, the SP can serve the requests at ENs closer to the users. We envision the emergence of an EC market managed by a Telco, a cloud provider (e.g., Amazon), or a third-party [3], [4], [15]. Indeed, numerous EC markets are currently being constructed by big companies and startups. The SP is assumed to have access to a portal listing various types of ENs in the market. Based on different factors such as price and location, the SP will decide where to place the service and how much resource to buy from each EN.

We consider an EC system that consists of a set \mathcal{N} of N ENs and a set \mathcal{M} of M APs. Let i and j be the EN index and AP index, respectively. Also, denote by C_j the computing resource capacity of EN j (e.g., number of servers, number of virtual machines, number of vCPUs, or number of CPU cycles per second). Define p_0 and p_j as the price of one computing unit at the cloud and at EN j , respectively. In practice, the ENs can be geographically distributed in different locations that have different electricity prices. Furthermore, the ENs may come with different sizes, ownership, server types, and configurations. Thus, the computing resource prices can vary among the ENs. Similar to the previous literature [3], [4], [14]–[35], we only consider the network from the APs to the ENs and the cloud. Let $d_{i,0}$ and $d_{i,j}$ be the distance between AP i and the cloud, and between AP i and AP j , respectively. Fig. 2 illustrates the system model with 4 ENs and 5 APs. The service here is Google Maps, which is placed at EN1, EN2, and the cloud.

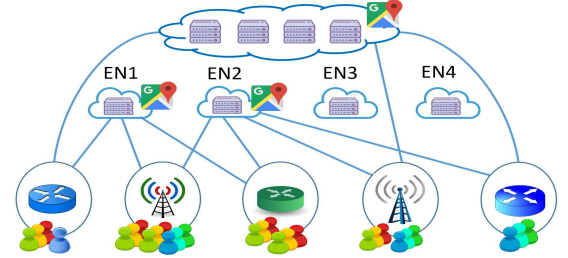


Fig. 2: System model

The SP is assumed to be a price-taker and have a budget B for operating the service at the edge and the cloud. The SP uses the budget to buy cloud and edge resources to serve the user requests during a fixed period of time (e.g., 30 minutes, few hours, or a day), with the goal of minimizing not only the resource procurement cost but also the total network delay of the requests. As mentioned in the introduction, to lower the network delay and reduce the data transmission, the SP can place the service on different ENs. Let z_j be a binary variable that equals to 1 if the SP decides to place the service onto EN j and 0 otherwise. Also, let z_j^0 be a binary indicator that equals to 1 if the service is available at EN j at the beginning.

If the SP wants to place the service onto EN j that does not have the service installed at the beginning of the scheduling horizon, we need to download the software and data of the service from a remote server or nearby ENs and install it onto EN j . This will incur a cost f_j that can be calculated as follows. First, denote by \mathcal{F} the set of ENs that have the

service at the beginning, i.e., $\mathcal{F} = \{j \mid z_j^0 = 1\}$. Let $f_{j,0}$ be the cost of installing and downloading the service from the cloud to EN j . Similarly, $f_{j,j'}$ is the cost of installing and downloading the service from EN j' to EN j . Typically, $f_{j,0} > f_{j,j'}$ for all j and j' because the distance between two ENs is much shorter than the distance between the cloud and an EN. We have:

$$f_j = \min \left\{ f_{j,0}, \min_{j' \mid j' \in \mathcal{F}} f_{j,j'} \right\}. \quad (1)$$

Let s_j be the cost of storing the service at EN j . Also, define y_0 and y_j as the amount of computing resource purchased from the cloud and EN j , respectively. The request arrival rate (i.e., traffic demand, workload) of the service at AP i is denoted by λ_i . Given the set of procured edge and cloud resources, the SP decides how to optimally divide the workload in different areas to the ENs and the cloud for processing to minimize the total network delay. Define $x_{i,0}$ as the portion of workload at AP i to be routed to the cloud, and $x_{i,j}$ as the workload at AP i assigned to EN j . Obviously, the SP prefers to have the requests processed by an EN closer to them rather than the remote cloud. To ensure the service quality, the SP may impose an upper bound D^m on the average network delay. A lower average delay implies that more requests are processed at the edge. The main notations are summarized in Table I.

III. PROBLEM FORMULATION

In this section, we first present a deterministic formulation of the service placement, resource procurement, and request scheduling problem, which is then extended to a two-stage robust formulation to deal with demand uncertainty.

A. Deterministic Formulation

In the deterministic model, the SP jointly optimizes the service placement, sizing, and workload allocation decisions when the traffic demand is assumed to be known exactly.

1) *Objective Function*: In this paper, we are interested in minimizing the total cost of the SP as follows:

$$\underset{x, y, z}{\text{minimize}} \mathcal{C} = \mathcal{C}^p + \mathcal{C}^s + \mathcal{C}^e + \mathcal{C}^c + \mathcal{C}^d, \quad (2)$$

where \mathcal{C}^p is the placement cost, \mathcal{C}^s is the storage cost, \mathcal{C}^e is the cost of purchasing edge computing resource, \mathcal{C}^c is the cloud resource procurement cost, and \mathcal{C}^d is the network delay cost. Also, we have $z = (z_1, z_2, \dots, z_N)$, $y = (y_0, y_1, \dots, y_N)$, $x = \{x_0, x_1, \dots, x_N\}$, $x_0 = (x_{1,0}, x_{2,0}, \dots, x_{M,0})$, and $x_j = (x_{1,j}, x_{2,j}, \dots, x_{M,j})$, $\forall j$.

As explained in the system model section, the service placement cost \mathcal{C}_j^p is the total cost of downloading and installing the service at EN j , which can be expressed as:

$$\mathcal{C}_j^p = f_j(1 - z_j^0)z_j, \quad \forall j. \quad (3)$$

Clearly, if the service is available at EN j at the beginning (i.e., $z_j^0 = 1$), the service placement cost becomes zero. When the service is placed at EN j but it is not available at the node at the beginning (i.e., $z_j = 1$ and $z_j^0 = 0$), \mathcal{C}_j^p is equal to f_j . Additionally, if the SP decides to run the service at EN j ($z_j = 1$), the cost of storing the service data at EN j is:

$$\mathcal{C}_j^s = s_j z_j, \quad \forall j. \quad (4)$$

The edge resource procurement cost at EN j is equal to the amount of purchased resource y_j multiplied by the resource price at the EN, i.e., we have:

$$\mathcal{C}_j^e = p_j y_j, \quad \forall j. \quad (5)$$

Similarly, the cloud resource procurement cost \mathcal{C}^c is $p_0 y_0$. In addition, the total network delay of all the service requests is:

$$d^{\text{tot}} = \sum_i d_{i,0} x_{i,0} + \sum_{i,j} d_{i,j} x_{i,j}. \quad (6)$$

Thus, the total network delay cost \mathcal{C}^d is βd^{tot} . Overall, the goal of SP is to minimize the following objective function:

$$\begin{aligned} \mathcal{C} = & \sum_j f_j(1 - z_j^0)z_j + \sum_j s_j z_j + p_0 y_0 + \sum_j p_j y_j \\ & + \beta \left(\sum_i d_{i,0} x_{i,0} + \sum_{i,j} d_{i,j} x_{i,j} \right). \end{aligned} \quad (7)$$

The SP can vary the delay cost parameter β to control the tradeoff between the total expenses of the SP and the total network delay of the requests (i.e., between cost and service quality). The weight β reflects the SP's attitude towards the network delay. Clearly, a larger β indicates that the SP is more delay-sensitive and willing to spend more to lower the delay. Note that the delay of each request includes the transmission delay, propagation delay (network delay), and processing delay at the cloud or an EN. In this work, we assume that each request is assigned a fixed amount of computing resource w and transmission bandwidth. Thus, the processing delay and the transmission delay (i.e., the request size divided by the bandwidth) are fixed. Hence, for simplicity, we consider the network delay only.

Additionally, it is straightforward to consider other costs such as bandwidth cost, which would discourage sending workload to the cloud, with minor modifications. We are now ready to describe all the constraints of the underlying optimization problem.

2) *Budget Constraint*: The total expense should not exceed the budget of the SP. Thus, we have the following constraint:

$$\sum_j f_j(1 - z_j^0)z_j + \sum_j s_j z_j + \sum_j p_j y_j + p_0 y_0 \leq B. \quad (8)$$

3) *Reliability Constraint*: To enhance the service reliability, the SP may want to place the service on at least a minimum number of r^{\min} ENs since link/node failures can occur unexpectedly. Hence, we can impose:

$$\sum_j z_j \geq r^{\min}. \quad (9)$$

4) *Workload Allocation Constraints*: The service requests arriving at each AP must be allocated to either the remote cloud or the ENs. Hence, we have:

$$x_{i,0} + \sum_j x_{i,j} = \lambda_i, \quad \forall i. \quad (10)$$

5) *Capacity Constraints*: The amount of computing resource y_0 and y_j purchased at the cloud and each EN j should be sufficient to serve the resource demand of all requests assigned to the cloud and the EN. Also, the SP buys resource only from the ENs that have the service installed (i.e., $z_j = 1$).

Furthermore, the amount of resource purchased from each EN j cannot exceed the capacity C_j of the EN. Thus:

$$w \sum_i x_{i,0} \leq y_0 \quad (11)$$

$$w \sum_i x_{i,j} \leq y_j, \quad \forall j \quad (12)$$

$$y_j \leq z_j C_j, \quad \forall j. \quad (13)$$

6) *Delay Constraint:* In order to ensure a certain service quality for their users, the SP may require the average network delay (d^{avg}) of the requests does not exceed a certain maximum delay threshold D^m . The average network delay is:

$$d^{\text{avg}} = \frac{\sum_i d_{i,0} x_{i,0} + \sum_{i,j} d_{i,j} x_{i,j}}{\sum_i \lambda_i} \quad (14)$$

Hence, $d^{\text{avg}} \leq D^m$ can be rewritten as:

$$\sum_i d_{i,0} x_{i,0} + \sum_{i,j} d_{i,j} x_{i,j} \leq D^m \sum_i \lambda_i. \quad (15)$$

7) *Constraints on Variables:* The service placement indicator z_j is a binary variable. Also, the workload allocation x and resource procurement y must be non-negative. Thus:

$$x_{i,0} \geq 0, \quad \forall i; \quad x_{i,j} \geq 0, \quad \forall i, j \quad (16)$$

$$z_j \in \{0, 1\}, \quad \forall j; \quad y_0 \geq 0; \quad y_j \geq 0, \quad \forall j. \quad (17)$$

Overall, the SP aims to solve the following problem:

$$\begin{aligned} \text{(Deter)} \quad & \underset{x, y, z}{\text{minimize}} \quad \mathcal{C} \\ & \text{subject to} \quad (7) - (17). \end{aligned}$$

This is an MILP that can be solved efficiently using existing MILP solvers. Note that our model can be easily extended to capture other system and design constraints. For instance, we may consider multiple resource types (e.g., RAM, CPU, bandwidth) instead of only computing resource. The SP may be enforced to buy an integer quantity of computing units from each EN rather than a continuous amount y_j , which can be easily handled using a unary or binary expansion.

In summary, given the system parameters such as the network topology, the downloading and installation costs, the resource price and capacity at each EN, the budget, and the delay penalty cost, the SP solves the MILP problem (Deter) to find an optimal service placement, resource procurement, and workload allocation solution.

B. Uncertainty Modeling

In the deterministic model, the traffic demand is assumed to be known exactly at the time of making the service placement and sizing decision. In other words, the SP assumes that the actual demand is the same as the forecast one, which is then used as input to the deterministic problem. However, the exact demand in each area typically cannot be accurately predicted at the time of making the strategic decision. Thus, how to properly capture the uncertainties in the decision making process is a crucial task.

In RO, uncertain parameters are modeled through uncertainty sets, which express an infinite number of scenarios. A well constructed uncertainty set should be computationally tractable and balance robustness and conservativeness of the

robust solution [8]. In practice, the polyhedral uncertainty set is a natural and popular choice for representing uncertainties in the RO literature [8], [12], [13]. In particular, to construct a polyhedral uncertainty set, the SP would need to specify intervals expressing the uncertain demand at every AP, and a parameter to control the degree of conservativeness.

Define $\lambda = (\lambda_1, \lambda_2, \dots, \lambda_M)$ and $\lambda^f = (\lambda_1^f, \lambda_2^f, \dots, \lambda_M^f)$ as the actual demand vector and the forecast demand vector, respectively. Note that λ_i^f is also called the nominal value of the uncertain demand λ_i . Additionally, let $\hat{\lambda} = (\hat{\lambda}_1, \hat{\lambda}_2, \dots, \hat{\lambda}_M)$, where $\hat{\lambda}_i$ is the maximum demand deviation, which can be understood as the maximum forecasting error of the uncertain demand at AP i , $\forall i$. Thus, $[\lambda_i^f - \hat{\lambda}_i, \lambda_i^f + \hat{\lambda}_i]$ represents the uncertain demand at AP i . The polyhedral uncertainty set can be defined as follows:

$$\mathcal{D}(\lambda^f, \hat{\lambda}, \Gamma) = \left\{ \begin{aligned} & \lambda_i = \lambda_i^f + g_i \bar{\lambda}_i, \quad \forall i; \quad g_i \in [-1, 1], \quad \forall i \\ & \sum_i |g_i| \leq \Gamma \end{aligned} \right\}, \quad (18)$$

where Γ is the budget of uncertainty, which can vary in the continuous interval $[0, M]$. The form of this uncertainty set is widely used in the RO literature [8], [12], [13]. This set contains the lower and upper bounds of the uncertain parameters and the bound of the linear combination of the uncertain parameters. These information can be extracted by learning from historical data. Indeed, a more general polyhedron can also be accommodated by the RO approach.

The actual demand λ_i can take any value in the range of $[\lambda_i^f - \hat{\lambda}_i, \lambda_i^f + \hat{\lambda}_i]$. However, in practice, it is not likely that all the actual demands are simultaneously close to the corresponding lower bounds or upper bounds. This observation is captured by the uncertainty budget Γ . A larger value of Γ implies a larger uncertainty set and a more robust solution. However, the solution is also more conservative to protect the system against a higher degree of uncertainty. Therefore, Γ can be used to adjust the robustness against the conservative level of the solution. When $\Gamma = 0$, the actual demand is equal to the forecast demand and a robust model becomes a deterministic model without considering demand uncertainty. When $\Gamma = M$, we simply consider all possible realizations of the uncertain demand λ_i in the interval of $[\lambda_i^f - \hat{\lambda}_i, \lambda_i^f + \hat{\lambda}_i]$, and \mathcal{D} becomes a box uncertainty set. Hence, the polyhedral uncertainty set is less conservative compared to the box uncertainty set.

C. Robust Optimization Formulation

In the static (single-stage) robust optimization model, the service placement, sizing, and workload allocation decisions are made simultaneously before observing the actual realization of the demand. Based on the RO theory [8], the robust service placement and sizing problem can be formulated as:

$$\begin{aligned} \min_{(x, y, z) \in \mathcal{S}(x, y, z)} \quad & \max_{\lambda \in \mathcal{D}} \sum_j f_j (1 - z_j^0) z_j + \sum_j s_j z_j + p_0 y_0 \\ & + \sum_j p_j y_j + \beta \left\{ \sum_i d_{i,0} x_{i,0} + \sum_{i,j} d_{i,j} x_{i,j} \right\} \end{aligned} \quad (19)$$

subject to

$$x_{i,0} + \sum_j x_{i,j} \geq \lambda_i, \quad \forall i, \lambda \in \mathcal{D} \quad (20)$$

$$\sum_i d_{i,0}x_{i,0} + \sum_{i,j} d_{i,j}x_{i,j} \leq D^m \sum_i \lambda_i, \lambda \in \mathcal{D}, \quad (21)$$

where $\mathcal{S}_{(X,Y,Z)}$ is the set of constraints on the placement, sizing, and workload allocation variables. These constraints are given in the deterministic model. The RO model aims to minimize the total cost of the SP under the worst-case demand scenario. Also, all the constraints related to uncertain parameters should be satisfied for any potential realization of these parameters within the uncertainty set.

Note that in the deterministic formulation, the workload allocation constraints (10) can be written as either equalities or inequalities since inequalities become equalities at the optimality for the cost minimization objective. Also, equalities related to uncertainties are meaningless in the RO approach [8] since the equality constraints cannot be satisfied for every demand scenario in the uncertainty set. Hence, the workload allocation constraints is written in form of inequalities as in (20). Due to space limitation, we do not present the solution approach here and refer to *Appendix B* for more details.

Overall, the static single-stage robust model includes two levels, as illustrated in Fig. 3. The first level represents the decision-making problem of the SP prior to the uncertainty realization and seeks to minimize objective function value (i.e., the total cost of the SP). The second level represents the uncertainty realization in the worst case within the uncertainty set \mathcal{D} and aims to maximize the objective function value. Given the uncertainty set and the system parameters as the input to the decision-making problem, the SP solves the RO model (19)-(21) to determine a robust optimal service placement and sizing solution.

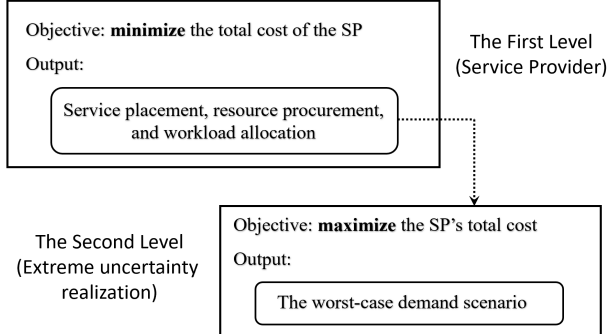


Fig. 3: The RO model for edge service placement and sizing

D. Two-Stage Adaptive Robust Formulation

Unlike the RO model where all decisions are made simultaneously in a single stage, the ARO model includes two stages. In particular, the service placement and the resource sizing are the first-stage decision variables. Given the first-stage decisions, the workload allocation decisions (i.e., operation decisions) are determined as an optimal solution to the second-stage problem (i.e., the recourse problem). Note that the first-stage decisions are made without the knowing the uncertain parameters while the recourse decisions are made based on

the revealed uncertainties. Define $h_j = f_j(1 - z_j^0) + s_j$, $\forall j$. The two-stage adaptive robust model can be formulated as:

$$\min_{(y,z) \in \mathcal{S}_{(Y,Z)}} \left\{ \sum_j h_j z_j + \sum_j p_j y_j + p_0 y_0 \right. \quad (22)$$

$$\left. + \max_{\lambda \in \mathcal{D}} \min_{x \in \mathcal{F}(y,\lambda)} \beta \left(\sum_i d_{i,0}x_{i,0} + \sum_{i,j} d_{i,j}x_{i,j} \right) \right\},$$

where:

$$\mathcal{S}_{(Y,Z)} = \left\{ \begin{array}{l} \sum_j z_j \geq r^{\min}; \quad y_j \leq z_j C_j, \quad \forall j, \\ \sum_j h_j z_j + \sum_j p_j y_j + p_0 y_0 \leq B, \\ z_j \in \{0, 1\}; \quad y_0 \geq 0; \quad y_j \geq 0, \quad \forall j \end{array} \right\} \quad (23)$$

$$\mathcal{F}(y, \lambda) = \left\{ \begin{array}{l} x \in \mathcal{S}_X; \quad x_{i,0} + \sum_j x_{i,j} = \lambda_i, \quad \forall i, \\ w \sum_i x_{i,0} \leq y_0; \quad w \sum_i x_{i,j} \leq y_j, \quad \forall j, \\ \sum_i d_{i,0}x_{i,0} + \sum_{i,j} d_{i,j}x_{i,j} \leq D^m \sum_i \lambda_i \end{array} \right\} \quad (24)$$

$$\mathcal{S}_X = \left\{ \begin{array}{l} x_{i,0} \geq 0, \quad \forall i; \quad x_{i,j} \geq 0, \quad \forall i, j \end{array} \right\}. \quad (25)$$

Note that $\mathcal{S}_{(Y,Z)}$ represents the constraints on the service placement and sizing variables, and $\mathcal{F}(y, \lambda)$ is the set of feasible workload allocation solutions for a fixed resource procurement decision y and demand realization λ . The optimal workload allocation aims to minimize the total delay cost in the worst-case scenario of the demands. The two-stage robust service placement and sizing above is inherently a trilevel (mix-max-min) optimization model, which is difficult to solve.

Fig. 4 illustrates the ARO model. The first level represents the decision-making problem of the SP before the uncertainty realization and seeks to minimize the SP's total cost. The second level represents the worst-case uncertainty realization, which tries to degrade the service quality by maximizing the total network delay. Finally, the third level represents the workload allocation decisions to mitigate the effects of the realized uncertainty. The workload allocation problem aims to minimize the total delay cost.

IV. SOLUTION APPROACH

In this section, we develop an iterative algorithm based on the column and constraint generation (CCG) procedure [13] to solve the formulated two-stage robust service placement and sizing problem (22). In particular, the developed algorithm is implemented in a master-subproblem framework that decomposes the problem into a master problem and a bilevel max-min subproblem. The optimal value of the master problem in each iteration provides a lower bound while the optimal solution to the subproblem helps us compute an upper bound of the original two-stage robust problem (22). The algorithm iteratively solves an updated master problem and an updated subproblem in each iteration until convergence.

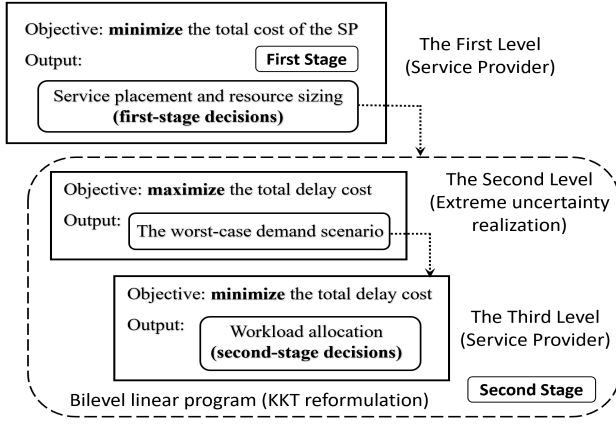


Fig. 4: The proposed tri-level ARO model

First, it can be shown that the two-stage robust model (22) can be transformed into an equivalent mixed integer program built on the collection of extreme points of the uncertainty set \mathcal{D} . It can be explained intuitively as follows. Assume that the problem (22) as well as the innermost minimization problem in (22) are feasible. Then, we can rewrite the second-stage bilevel problem as a max-max problem (i.e., simply a maximization problem) over λ and the set of dual variables associated with the constraints of the innermost minimization problem. Since this maximization problem is optimized over two disjoint polyhedrons, it always has an optimal solution combining extreme points of these two polyhedrons [36]. Therefore, the optimal solution to the second-stage problem always occurs an extreme point of the polyhedron \mathcal{D} .

Define K as the number of extreme points of the uncertainty set \mathcal{D} . Also, let $\mathbb{D} = \{\lambda^1, \lambda^2, \dots, \lambda^K\}$ be the set of extreme points (i.e., extreme demand scenarios) of \mathcal{D} , where $\lambda^l = \{\lambda_1^l, \lambda_2^l, \dots, \lambda_M^l\}$ is the l -th extreme point. Therefore, the ARO model (22) is equivalent to:

$$\min_{(y,z) \in \mathcal{S}_{(Y,Z)}} \left\{ \sum_j h_j z_j + \sum_j p_j y_j + p_0 y_0 \right. \quad (26)$$

$$\left. + \max_{\lambda \in \mathbb{D}} \min_{x \in \mathcal{F}(y,\lambda)} \beta \left(\sum_i d_{i,0} x_{i,0} + \sum_{i,j} d_{i,j} x_{i,j} \right) \right\}.$$

Clearly, this problem can be transformed into the following equivalent MILP by enumerating all the extreme points in \mathbb{D} :

$$\min_{\eta, (y,z) \in \mathcal{S}_{(Y,Z)}} \sum_j h_j z_j + \sum_j p_j y_j + p_0 y_0 + \eta \quad (27)$$

subject to

$$\eta \geq \beta \left\{ \sum_i d_{i,0} x_{i,0}^l + \sum_{i,j} d_{i,j} x_{i,j}^l \right\}, \quad \forall l \leq K \quad (28)$$

$$x^l \in \mathcal{F}(y, \lambda^l), \quad \forall l \leq K. \quad (29)$$

For a large polyhedral uncertainty set as in (18), obtaining the optimal solution to the reformulated large-scale MILP above, which needs to enumerate all the possible extreme demand scenarios, may be not practically feasible. This motivates the iterative solution based on the CCG method [13]. Specifically, instead of solving the full problem (27)-(29) for

all extreme points in the uncertainty set, we only solve this problem for a subset of \mathbb{D} , which obviously provides a valid relaxation of this problem and give us a lower bound (LB). Therefore, we can obtain stronger LBs by gradually adding non-trivial demand scenarios to the relaxed problem. This is indeed the core idea behind the CCG method, which expands a subset of \mathbb{D} gradually and add an additional variable x^k in each iteration k . Furthermore, an optimal solution to the second-stage problem for a fixed (y, z) clearly provides an upper bound (UB) of the two-stage robust problem (22).

In the following, we first describe the master problem that is a relaxation of the problem (27)-(29). Then, we elaborate how to solve the subproblem (i.e., the second-stage problem) given the first-stage decision. Finally, we present the iterative algorithm for solving the two-stage robust service placement and sizing problem in a master-subproblem framework.

A. Master Problem

The master problem (**MP**) at iteration k is given as:

$$\min_{y,z,\eta} \sum_j h_j z_j + \sum_j p_j y_j + p_0 y_0 + \eta \quad (30)$$

subject to

$$\eta \geq \beta \left\{ \sum_i d_{i,0} x_{i,0}^l + \sum_{i,j} d_{i,j} x_{i,j}^l \right\}, \quad \forall l \leq k \quad (31)$$

$$x_{i,0}^l + \sum_j x_{i,j}^l = \lambda_i^{*,l}, \quad \forall l \leq k \quad (32)$$

$$w \sum_i x_{i,0}^l \leq y_0, \quad \forall l \leq k; \quad w \sum_i x_{i,j}^l \leq y_j, \quad \forall j, \forall l \leq k \quad (33)$$

$$\sum_i d_{i,0} x_{i,0}^l + \sum_{i,j} d_{i,j} x_{i,j}^l \leq D^m \sum_i \lambda_i^{*,l}, \quad \forall l \leq k \quad (34)$$

$$x_{i,0}^l \geq 0, \quad x_{i,j}^l \geq 0, \quad \forall l \leq k; \quad (y, z) \in \mathcal{S}_{(Y,Z)}; \quad \eta \in \mathbb{R}, \quad (35)$$

where $\{\lambda^{*,1}, \lambda^{*,2}, \dots, \lambda^{*,k}\}$ is the set of optimal solutions to the subproblem in all previous iterations up to iteration k . Also, $\lambda^{*,l} = \{\lambda_1^{*,l}, \lambda_2^{*,l}, \dots, \lambda_M^{*,l}\}, \forall l$. The optimal solution to this master problem includes the optimal placement $(z_j^{*,k+1}, \forall j)$, sizing $(y_0^{*,k+1}, y_j^{*,k+1}, \forall j)$, delay cost $(\eta^{*,k+1})$, and workload allocation $x^{*,l}, \forall l \leq k$. Then, the optimal sizing decisions $y_0^{*,k+1}$ and $y_j^{*,k+1}, \forall j$ will serve as input to the subproblem in Section IV-B. Indeed, the master problem at iteration k corresponds to k extreme points of the uncertainty set \mathcal{D} . Therefore, because each **MP** contains only a subset of constraints of the original two-stage RO formulation (27)-(29), the optimal solution to an **MP** provides a LB of the original problem. We also achieve a stronger LB in every iteration since each new iteration adds more constraints to the **MP**. Thus:

$$LB = \sum_j h_j z_j^{*,k+1} + \sum_j p_j y_j^{*,k+1} + p_0 y_0^{*,k+1} + \eta^{*,k+1}. \quad (36)$$

B. Reformulation of the Subproblem

The max-min subproblem is indeed a bilevel optimization problem, which is difficult to solve. To this end, we show how to reformulate the subproblem as a MILP problem that can be

solved globally using MILP solvers. Specifically, given y , the subproblem (**SP**) is:

$$\mathcal{Q}(y) = \max_{\lambda \in \mathcal{D}} \min_{x \in \mathcal{F}(y, \lambda)} \beta \left\{ \sum_i d_{i,0} x_{i,0} + \sum_{i,j} d_{i,j} x_{i,j} \right\} \quad (37)$$

From (24), the inner minimization problem can be written as:

$$\min_x \beta \left\{ \sum_i d_{i,0} x_{i,0} + \sum_{i,j} d_{i,j} x_{i,j} \right\} \quad (38)$$

subject to

$$w \sum_i x_{i,0} \leq y_0, \quad (\pi_0) \quad (39)$$

$$w \sum_i x_{i,j} \leq y_j, \quad \forall j \quad (\pi_j) \quad (40)$$

$$\sum_i d_{i,0} x_{i,0} + \sum_{i,j} d_{i,j} x_{i,j} \leq D^m \sum_i \lambda_i, \quad (\mu) \quad (41)$$

$$x_{i,0} + \sum_j x_{i,j} = \lambda_i, \quad \forall i, \quad (\sigma_i) \quad (42)$$

$$x_{i,0} \geq 0, \quad \forall i \quad (\xi_{i,0}) \quad (43)$$

$$x_{i,j} \geq 0, \quad \forall i, j, \quad (\xi_{i,j}) \quad (44)$$

where $\pi_0, \pi_j, \mu, \sigma_i, \xi_{i,0}, \xi_{i,j}$ are the dual variables associated with constraints (39)-(44), respectively. Also, y are the optimal sizing solution to the latest **MP**, i.e., at iteration k , we have $y_0 = y_0^{*,k+1}$ and $y_j = y_j^{*,k+1}, \forall j$.

Based on the Karush–Kuhn–Tucker (KKT) conditions [45], we can infer that given (y, λ) , the optimal solution x to the innermost problem (38)-(44) is any of the feasible solutions to the set of constraints (46)-(51). Please refer to *Appendix C* for more details. Hence, the **SP** (37) is equivalent to the following problem with complementary constraints:

$$\max_{x, \lambda, \pi_0, \pi_j, \mu, \sigma_i} \beta \left\{ \sum_i d_{i,0} x_{i,0} + \sum_{i,j} d_{i,j} x_{i,j} \right\} \quad (45)$$

subject to

$$0 \leq \beta d_{i,0} + w \pi_0 + \mu d_{i,0} - \sigma_i \perp x_{i,0} \geq 0, \quad \forall i \quad (46)$$

$$0 \leq \beta d_{i,j} + w \pi_j + \mu d_{i,j} - \sigma_i \perp x_{i,j} \geq 0, \quad \forall i, j \quad (47)$$

$$0 \leq (y_0 - w \sum_i x_{i,0}) \perp \pi_0 \geq 0 \quad (48)$$

$$0 \leq (y_j - w \sum_i x_{i,j}) \perp \pi_j \geq 0, \quad \forall j \quad (49)$$

$$0 \leq (D^m \sum_i \lambda_i - \sum_i d_{i,0} x_{i,0} - \sum_{i,j} d_{i,j} x_{i,j}) \perp \mu \geq 0 \quad (50)$$

$$x_{i,0} + \sum_j x_{i,j} = \lambda_i, \quad \forall i \quad (51)$$

$$\lambda_i = \lambda_i^f + g_i \hat{\lambda}_i, \quad \forall i; \quad \sum_i t_i \leq \Gamma; \quad t_i \leq 1, \quad \forall i \quad (52)$$

$$-t_i + g_i \leq 0, \quad \forall i; \quad t_i + g_i \geq 0, \quad \forall i, \quad (53)$$

where the last two constraints represent the uncertainty set \mathcal{D} . Note that a complimentary constraint $0 \leq x \perp \pi \geq 0$ means $x \geq 0, \pi \geq 0$ and $x \pi = 0$. Thus, it is a nonlinear constraint. Fortunately, this nonlinear complimentary constraint can be transformed into equivalent exact linear constraints by using

the Fortuny-Amat transformation [46]. Specifically, the complementarity condition $0 \leq x \perp \pi \geq 0$ is equivalent to the following set of mixed-integer linear constraints:

$$\begin{aligned} x &\geq 0; \quad x \leq (1-u)M \\ \pi &\geq 0; \quad \pi \leq uM, \quad u \in \{0, 1\}, \end{aligned} \quad (54)$$

where M is a sufficiently large constant. By applying this transformation to all the complementary constraints (46)-(50), we obtain an MILP that is equivalent to the subproblem (37). The explicit form of this MILP is given in *Appendix D*. Thus, the subproblem can be solved using an MILP solver.

Denote by $(\lambda^{*,k+1}, x^{*,k+1})$ the optimal solution to the **SP** at iteration k . The solution to each **SP** helps us determine an UB to the original two-stage RO problem. Specifically, we have:

$$UB = \min \{UB, UB^{k+1}\}, \quad (55)$$

$$\begin{aligned} UB^{k+1} = & \sum_j h_j z_j^{*,k+1} + \sum_j p_j y_j^{*,k+1} + p_0 y_0^{*,k+1} \\ & + \beta \left(\sum_i d_{i,0} x_{i,0}^{*,k+1} + \sum_{i,j} d_{i,j} x_{i,j}^{*,k+1} \right). \end{aligned} \quad (56)$$

Also, $\lambda^{*,k+1}$ is used as input to the **MP** in the next iteration.

C. Algorithm

Based on the description of the master problem and the subproblem, we are now ready to present the CCG-based iterative algorithm for solving the formulated two-stage robust service placement and sizing problem (22) as shown in **Algorithm 1**.

Algorithm 1 TWO-STAGE ADAPTIVE ROBUST ALGORITHM

- 1: Initialization: set $k = 1$, $LB = -\infty$, and $UB = +\infty$.
- 2: **repeat**
- 3: Solve the following **MP**.

$$\begin{aligned} \min_{\eta, (y, z) \in \mathcal{S}(Y, Z)} & \sum_j h_j z_j + \sum_j p_j y_j + p_0 y_0 + \eta \quad (57) \\ \text{subject to} & \quad x^l \in \mathcal{F}(y, \lambda^l), \quad \forall l \leq k \end{aligned}$$

$$\eta \geq \beta \left\{ \sum_i d_{i,0} x_{i,0}^l + \sum_{i,j} d_{i,j} x_{i,j}^l \right\}, \quad \forall l \leq k.$$

Obtain an optimal solution $(\eta^{*,k+1}, z^{*,k+1}, y^{*,k+1}, x^{*,1}, \dots, x^{*,k})$ and update LB according to (36).

- 4: Solve **SP** (37) with $y = y^{*,k+1}$ to obtain the worst-case demand $\lambda^{*,k+1}$ given y and update UB following (55).
 - 5: Update $\lambda^{k+1} = \lambda^{*,k+1}$, and $k := k + 1$.
 - 6: **until** $\frac{UB-LB}{UB} \leq \epsilon$
 - 7: Output: optimal placement and sizing decisions (z^*, y^*) .
-

Different from [13], we consider the extreme scenario with the maximum total demand in the first iteration. In particular, without loss of generality, let λ^1 be the extreme demand scenario in \mathcal{D} with the maximum total demand. Specifically, $\lambda^1 = \{\lambda_1^1, \dots, \lambda_M^1\}$ can be computed as an optimal solution to the following optimization problem:

$$\begin{aligned} \max_{g, \lambda} & \sum_i \lambda_i \\ \text{s.t.} & \quad \lambda_i = \lambda_i^f + g_i \hat{\lambda}_i, \quad \forall i; \quad -1 \leq g_i \leq 1, \quad \forall i; \quad \sum_i |g_i| \leq \Gamma. \end{aligned}$$

Indeed, λ^1 can be found analytically by sorting the demand deviations $\hat{\lambda}_i$ in descending order and set g_i associated with the $\lfloor \Gamma \rfloor$ largest demand deviations to be 1 and g_i of the next largest λ_i to be $\Gamma - \lfloor \Gamma \rfloor$. Note that the ARO model (22) is equivalent to the problem (27)-(29) whose constraints enumerate over all extreme points of \mathcal{D} , including λ^1 . By considering λ^1 in the first iteration, we have $y_0 + \sum_j y_j \geq w \sum_i (x_{i,0}^1 + \sum_j x_{i,j}^1) = w \sum_i \lambda_i^1$. Hence, $y_0 + \sum_j y_j \geq w \sum_i \lambda_i^1, \forall i \leq K$. As a result, the total resource purchased from the cloud and the ENs is always sufficient to serve every realization of the demand.

Since new constraints related to λ^k are added to the MP (57) at every iteration k , the LB is improved (weakly-increasing) at every iteration. Also, by definition as in (55), the UB is non-increasing. Furthermore, as explained before, the worst-case demand in Step 4 is always an extreme point of the polyhedral uncertainty set \mathcal{D} . The set \mathbb{D} of extreme points is a finite set with K elements. Hence, we can prove that **Algorithm 1** converges to the optimal value of the original two-stage robust problem (22) in $O(K)$ iterations (see *Appendix E*).

V. NUMERICAL RESULTS

A. Simulation Setting

Since EC is still in its early stage and we are not aware of any public data for edge network topologies, similar to previous works [17], [39], we adopt the Barabasi-Albert model [41] to generate random a scale-free edge network topology with 100 nodes and the attachment rate of 2 [17]. Also, link delays are randomly generated in between 2 ms and 5 ms [42]. The network transmission delay between any two APs is the delay of the shortest path between them. Based on the generated topology, 80 nodes are chosen as APs and 20 nodes are chosen as ENs. The delay between each AP and the remote cloud is set to be 80 ms. Additionally, the forecast traffic arrival rate (i.e., demand) at each AP is randomly drawn from 1000 to 4000 requests per time unit [42], and the resource demand w of each service request is set to be 1 MHz [43].

Each EN is chosen randomly from the set of Amazon EC2 M5 instances [44]. Using the hourly price of a general purpose m5d.xlarge Amazon EC2 instance [44] as a reference, the resource price (\$ per vCPU per time unit) at the cloud is set to be 0.03 while the resource prices at the ENs are randomly generated from 0.04 to 0.06. Additionally, the service placement costs (f_j) and storage costs (s_j) at the ENs are randomly generated in the ranges of [0.2, 0.25] and [0.1, 0.12], respectively. The budget of the SP is set to be 100. We also assume that the service is not available on any EN at the beginning (i.e., $z_j^0 = 0, \forall j$).

For the sake of clarity in the figures and analysis, in the **base case**, we consider a small system with 20 APs and 5 ENs (i.e., $M = 20, N = 5$), which are selected randomly from the corresponding original sets of 80 APs and 20 ENs. Note that we also study the impacts of varying the number of APs and ENs later. In the base case, the maximum average delay D^m is set to be 30 ms, and the minimum number of edge servers r^{\min} is 2. Let α_i be the ratio between the maximum demand deviation $\hat{\lambda}_i$ and the forecast demand λ_i^f . Also, define $\beta_0 = \beta \sum_i \lambda_i^f$. In the base case, we set $\alpha_i = \alpha = 0.3, \forall i$, the uncertainty budget $\Gamma = 10$, and the delay penalty parameter $\beta_0 = 0.01$. This default setting is used in most of the

simulations unless mentioned otherwise. We implement all the algorithms in Matlab environment using CVX¹ and Gurobi².

B. Performance Evaluation

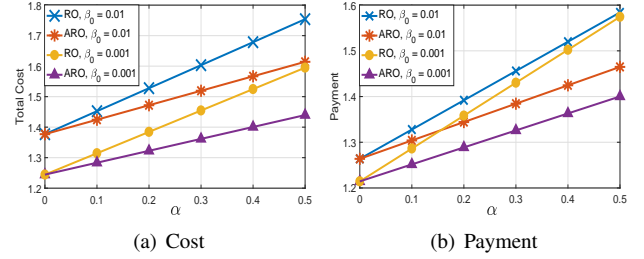


Fig. 5: Comparison between RO and ARO

1) Comparison between RO, ARO, and deterministic models: First, we compare the performance of the traditional RO approach and the ARO approach to verify that the ARO solution is less conservative than the RO solution. Specifically, Figs. 5(a) and 5(b) present the costs and payments, respectively, in the RO and ARO schemes under different values of the delay penalty β_0 . The payment is the total money spent for placing the service and buying resource, while the total cost is the value of the objective function that equals to the sum of the payment and the total network delay cost. As we can observe, the total cost as well as the payment produced by ARO is less than those of RO. Hence, these results indicate that the ARO solution is less conservative than the RO solution.

In addition, the total cost increases as the delay penalty cost increases (i.e., the SP is more delay-sensitive and willing to pay more to reduce the delay). Note that α is the ratio between the maximum demand deviation and the forecast demand, which can be understood as the **maximum forecast error** (e.g., $\alpha = 0.2$ implies an error of 20% of the forecast value). It can be seen that the costs and payments in the robust approaches increase as the forecast error α increases.

When $\alpha = 0$ (i.e., no uncertainty), the ARO and RO models become deterministic, and the robust solutions are the same as the deterministic solution. The cost and payment in the deterministic model (i.e., $\alpha = 0$) are lower than those in the robust models because the deterministic model assumes that the SP has perfect knowledge of the demand.

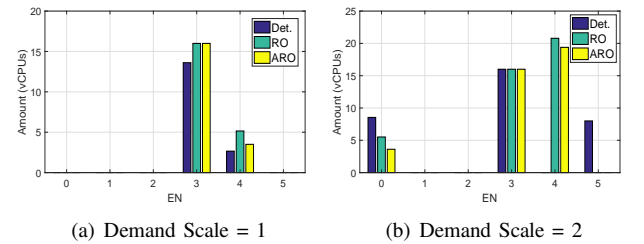


Fig. 6: Resource procurement comparison

Figs. 6(a) and 6(b) show the amount of resources procured from the ENs and the cloud (i.e., EN 0) in the deterministic scheme, RO scheme, and ARO scheme for a specific problem

¹<http://cvxr.com/cvx/>

²<https://www.gurobi.com/>

instance. The demand in each figure is equal to the demand in the base case multiplied by the demand scale factor. Clearly, in the deterministic model, the SP buys the lowest amount of resources since the demand is assumed to be exactly known. It can also be observed that the amount of procured resources in the ARO model is less than that in the RO model.

Note that the resource procurement solution depends on various factors such as the compute and storage prices at the cloud and the ENs, the capacity of each node, the network topology, the demand distribution in different areas, and the delay penalty. In general, the SP prefers to buy resources from ENs with lower prices and/or closer to high-demand areas. When the delay penalty parameter β_0 is small, the SP tends to purchase resources from low-price nodes, which may be far from high-demand areas. When β_0 is sufficiently large, the SP tends to buy resources from ENs in or near high-demand areas to reduce the overall delay, even though these ENs can be more expensive. It is because the delay penalty can outweigh other costs in this case.

For the problem instance in Figs. 6(a) and 6(b), EN1 and EN2 have the highest resource prices while the prices at EN3 are lowest. Furthermore, the demand is concentrated in the areas close to EN3–EN5. Hence, the SP prefers to buy more resources from EN3 and EN4, which offer the cheapest prices. In the normal demand condition in Fig. 6(a), the robust solutions suggest the SP to purchase all the compute resource of EN3, whose capacity is 16 vCPUs, and the remaining from EN4. In the deterministic model, the SP knows the exact demand in each area, and thus buys less resources. Also, the SP does not buy all resources of the cheapest node (EN3), but procures resources from EN4 to serve the demand near EN4 and EN5.

Although the cloud resource price is cheaper than the edge resource prices, the SP does not buy cloud resources due to the higher delay penalty cost at the cloud and the sufficiently low resource prices at EN3 and EN4. It is worth emphasizing that this does not always hold true and depends on the specific problem instance. For example, for the same problem instance except that the delay penalty parameter β_0 is set to be smaller, the SP may purchase a certain amount of computing resources from the cloud.

When the demand doubles as in Fig. 6(b), in the robust schemes, the SP buys sufficient resources from EN3 and EN4 to serve the demand in the areas near EN2–EN5. In the deterministic model, the demand is assumed to be known precisely. Thus, the SP installs the service and buys resources at EN5 even though the prices at EN5 are higher than those at EN3 and EN4. The difference between the robust solutions and the deterministic solution at EN4 and EN5 is because the robust solutions need to take the demand uncertainty into account. When β_0 is not too large and the resource prices at EN1 and EN2 are highest, the total resource and delay cost by serving requests at the cloud is lower than the total cost at EN1 and EN2. Hence, it is more economical for the SP to purchase resources from the cloud instead of EN1 and EN2.

2) *Comparison between RO, ARO, and deterministic approaches in the operation stage:* It is worth emphasizing that the main goals of the RO, ARO, and deterministic models presented throughout the paper are to identify the placement

and sizing decisions *before* knowing the actual demand. The robust approaches aim to hedge against any realization of the demand (i.e., robust against worst-case scenarios), while the deterministic approach uses the forecast demand to determine the optimal placement and sizing solution. However, the actual demand does not necessarily coincide with either the forecast demand or the worse-case demand scenario. Thus, it is important to evaluate the performance of these approaches in the actual operation stage when the demand is disclosed.

Indeed, the cost in the deterministic model should be acquired by solving it based initially on the forecast demand and then re-evaluating it under demand uncertainty. Specifically, we first solve the deterministic model using the forecast demand to obtain the optimal decision (y^*, z^*) . When the actual demand is revealed, the SP then solves the workload allocation problem using y^* as an input. Since y^* may not be sufficient to serve the actual demand, we allow dropping requests in the operation stage at a penalty cost v^p per percentage of unserved requests (see Appendix A for more details).

Thus, the actual cost of the deterministic model is the sum of the service placement and resource procurement costs before knowing the demand (i.e., first-stage cost) and the actual delay cost in the operation stage (i.e., second-stage cost). We apply similar procedures to the robust approaches since the actual demand is rarely the same as the worst-case demand scenario. In particular, the service placement and resource procurement costs are the costs in the first-stage before the demand is revealed. Given these decisions, the delay cost in the second-stage is re-computed when the actual demand is disclosed.

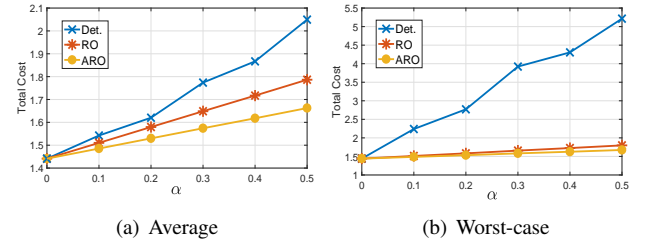


Fig. 7: Cost comparison under actual demand

We now compare the performance of the deterministic and robust approaches in terms of average cost and worst-case cost. First, we generate 100 demand scenarios within the uncertainty set. The average cost is the sum of the second-stage cost, which is averaged over 100 scenarios, and the first-stage provisioning cost. For the worst-case cost, the second-stage cost is the cost in the worst-case demand scenario (i.e., the scenario giving the maximum second-stage cost).

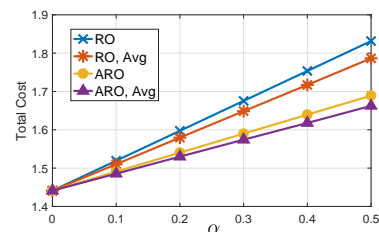


Fig. 8: Robust cost and actual cost

The average cost and the worst-case cost comparisons among these approaches are shown in Figs. 7(a) and 7(b), respectively. Here, we set $v^p = 40$ (e.g., the penalty will be 0.4 if 1% of requests are unserved). Since the deterministic method does not consider demand uncertainty, its cost is significantly higher than those of the robust schemes, especially in the worst-case scenario. Also, because the realized demand in the operation stage is usually not the worst-case demand scenario, the actual costs of the robust solutions are considerably lower than the optimal values of the objective functions (19) and (22) in the robust models, as can be seen in Fig. 8. This figure further confirms that ARO is less conservative than RO.

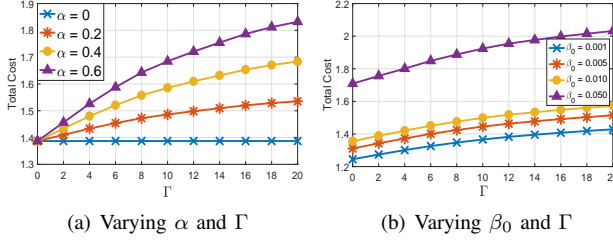


Fig. 9: The impact of the uncertainty set on the system performance

3) *Sensitivity Analysis*: We now study the impacts of different design parameters on the system performance. First, by definition, the uncertainty set is characterized by the maximum forecast error α and the uncertainty budget Γ . Figs. 9(a) and 9(b) show the impact of the uncertainty set on the optimal solution. As expected, the total cost increases as the uncertainty set \mathcal{D} enlarges (i.e., α increases and/or Γ increases). Note that the maximum value of Γ is 20 since we have 20 APs in the base case. Also, Fig. 9(b) suggests that the SP can lower the total cost by reducing the delay penalty parameter β_0 .

Figs. 10(a) and 10(b) illustrate the impact of number of ENs and number of APs, respectively, on the system performance. It is easy to see that when there are more ENs, the SP has more options to buy edge resources and allocate workload to closer ENs. Hence, the total cost of the SP decreases as N increases. Similarly, the total cost increases when there are more APs due to increasing total workload. Finally, the convergence property of the proposed algorithm is presented in Figs. 11(a) and 11(b) for certain problem instances. It can be seen that the algorithm converges very quickly towards the optimal solutions. Indeed, we conducted extensive numerical experiments which show that the algorithm typically converges in a few iterations (even just one or two iterations in some cases).

VI. RELATED WORK

Various aspects of EC have been studied over the last few years. A majority of the previous work has focused on the joint allocation of communication and computational resources for task offloading in wireless networks [37]. In [38], Stackelberg game and matching theory are combined to tackle the fog resource allocation problem. Reference [15] presents a primal-dual method for online matching edge resources to different service providers to maximize system efficiency. A cloudlet load balancing problem is formulated in [39] to minimize the maximum response time of offloaded tasks. R. Deng *et al.* [40]

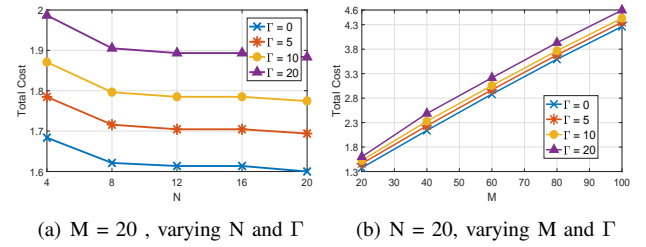


Fig. 10: The impact of M and N on the system performance

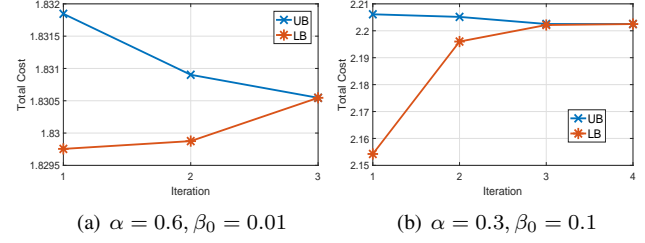


Fig. 11: Convergence property

propose a novel workload allocation model in a hybrid cloud-fog system to minimize energy cost under latency constraints. In [3], [4], a market equilibrium approach is employed to fairly and efficiently allocate edge resources to competing services. Unlike these works, we focus on the joint edge service placement and workload allocation problem.

A growing literature has focused on the optimal placement and activation of ENs. This line of research is complementary to our work where we examine the optimal placement of edge services and assume the set of ENs is given. In [16], the authors jointly optimize cloudlet placement and workload allocation to minimize the average network delay between mobile users and the cloudlets by placing a given number of cloudlets to some strategic locations. This model is extended in [17] to capture both network delay and computing delay at the cloudlets using queuing models. In [18], L. Ma *et al.* formulate a cloudlet placement and resource allocation problem, with the goal of minimizing the number of cloudlets while respecting the access delay requirements of users.

A ranking-based near optimal algorithm is presented in [20] for efficiently deploying cloudlets among numerous APs in an IoT network. Reference [21] aims to minimize the overall energy consumption subject to delay constraints by intelligently placing cloudlets on the network and allocating tasks to cloudlets and the public cloud. In [22], A. Ceselli *et al.* introduce a mobile edge cloud network planning framework that simultaneously considers cloudlet placement, assignment of APs to cloudlets, and traffic routing from and to the cloudlets, with the goal of minimizing the total installation costs of all network nodes. A MINLP formulation is proposed in [23] to determine optimal locations for cloudlet placement with minimum installation cost considering the capacity and latency constraints. Reference [24] presents a multi-objective optimization framework to minimize the service delay and the cloud's load by simultaneously identifying the optimal location, capacity, and number of ENs, as well as the optimal links between the ENs and the cloud.

Recently, service placement in EC has attracted a lot of

attention in the literature. In [25], a unified service placement and request dispatching framework is proposed to optimize the tradeoffs between the average latency of users' requests and the cost of service providers. In [26], the authors present an application image placement and task scheduling problem in a fog network with dedicated storage and computing servers to minimize the makespan. A constant-factor approximation algorithm is introduced in [28] to find a feasible service placement that maximizes the total user utility considering the heterogeneity of ENs and user locations. In [27], R. Yu *et al.* consider an IoT application provisioning problem that jointly optimizes application placement and data routing to support all data streams with both bandwidth and delay guarantees.

In [29], a joint application placement and workload allocation scheme is presented to minimize the response time of IoT application requests.

The work [30] introduces a fog service provisioning framework that dynamically deploys and releases applications on fog nodes to satisfy low latency and QoS requirements of the applications while minimizing the total system cost. The service entity placement problem for social virtual reality applications is examined in [19] to minimize the total system cost, including the cloudlet activation cost, the placement cost, the proximity cost, and the colocation cost, for deploying these applications at the edge. Joint optimization of access point selection and service placement is addressed in [31] to enhance user QoS by balancing the access delay, communication delay, and switching delay.

In [33], the authors jointly optimize service placement and request routing in MEC-enabled multi-cell networks to reduce the load of the centralized cloud considering the limited storage capacities of ENs and asymmetric bandwidth requirements of the services. In [14], a two-time-scale optimization framework is proposed to optimize service placement and request scheduling under multi-dimensional resource and budget constraints, in which request scheduling occurs at a smaller time scale and service placement occurs at a larger scale to reduce system instability. Most of the existing work on edge service placement does not consider uncertainties.

The resource allocation and provisioning problem under uncertainty in cloud/edge computing has also been studied in recent literature. In [34], T. Ouyang *et al.* formulate the dynamic service placement problem as a contextual multi-armed bandit problem and propose a Thompson-sampling based online learning algorithm to assist users to select an EN for offloading considering the tradeoff between latency and service migration cost. In the same line of research, due to the unknown benefit of placing edge service in a specific site, a combinatorial contextual bandit learning problem is presented in [35] to help an application provider decide the optimal set of ENs to host its service under the budget constraint.

In [5], [6], the authors employ the scenario-based stochastic programming approach to tackle different cloud resource provisioning problems that aims to minimize the total resource provisioning cost. Similarly, reference [7] formulates an energy-aware edge service placement as a multi-stage stochastic program with the objective of maximizing the QoS of the system under the limited energy budget of edge servers. In [9], [10], the authors propose different robust cloud resource

provisioning formulations using the standard RO method. Also, RO is utilized in [11] to jointly optimize radio and virtual machine resources in mobile edge computing.

Different from the existing literature, we formulate a new edge service placement problem from the perspective of a SP. Also, to deal with demand uncertainty, we propose a novel two-stage RO model for joint optimization of edge service placement, sizing, and workload allocation. To the best of our knowledge, this is the first work that employs two-stage adaptive robust optimization to tackle the edge service placement and resource procurement problem.

VII. CONCLUSION AND FUTURE WORK

In this paper, we introduced a novel two-stage RO model to help a SP decide an optimal service placement and sizing solution that can hedge against all possible realizations of the uncertain traffic demand within an uncertainty set. Given the placement and sizing decision in the first-stage, the workload allocation decisions are made in the second-stage after the uncertainty is revealed. The proposed robust model enables the SP to balance the tradeoff between the total operating cost and the service quality while taking demand uncertainty into account. Extensive numerical results were presented to demonstrate the advantages of the proposed scheme, which is less conservative compared to the RO approach and more robust compared to the deterministic approach.

There are several interesting directions for future work. First, we would like to study more efficient methods to speed up the computation of both the master problem and the subproblem. Second, instead of polyhedral sets, we would like to explore techniques to tackle more sophisticated and/or data-driven uncertainty sets (e.g., one that can better capture the highly dynamical and correlated uncertainty parameters). We also plan to extend the proposed model to the network slicing problem where a network operator optimizes the planning and operation of their edge network to serve multiple services with uncertain demand and different characteristics. Finally, we are interested in studying the impact of the placement and sizing decisions of the SP on the resource prices when there are multiple SPs in the system.

REFERENCES

- [1] M. Chiang and T. Zhang, "Fog and IoT: an overview of research opportunities," *IEEE Internet Things J.*, vol. 3, no. 6, pp. 854–864, Dec. 2016.
- [2] W. Shi, J. Cao, Q. Zhang, Y. Li, and L. Xu, "Edge computing: vision and challenges," *IEEE Internet Things J.*, vol. 3, no. 5, pp. 637–646, Oct. 2016.
- [3] D.T. Nguyen, L.B. Le, and V.K. Bhargava, "Price-based resource allocation for edge computing: a market equilibrium approach," *IEEE Trans. Cloud Comput.*, to be published.
- [4] D.T. Nguyen, L.B. Le, and V.K. Bhargava, "A market-based framework for multi-resource allocation in fog computing," *IEEE/ACM Trans. Netw.*, vol. 27, no. 3, pp. 1151–1164, June 2019.
- [5] S. Chaisiri, B. Lee, and D. Niyato, "Optimization of resource provisioning cost in cloud computing," *IEEE Trans. Serv. Comput.*, vol. 5, no. 2, pp. 164–177, Apr.–Jun. 2012.
- [6] S. Mireslamy, L. Rakai, M. Wang, and B. H. Far, "Dynamic cloud Resource Allocation Considering Demand Uncertainty," *IEEE Trans. Cloud Comput.* to be published.
- [7] H. Badri, T. Bahreini, D. Grosu, and K. Yang, "Energy-aware application placement in mobile edge computing: a stochastic optimization approach," *IEEE Trans. Parallel Distr. Syst.*, vol. 31, no. 4, pp. 909–922, Apr. 2020.

- [8] A. Ben-Tal, L. El Ghaoui, and A. Nemirovski, "Robust Optimization," Princeton, NJ, USA: Princeton Univ. Press, 2009.
- [9] S. Chaisiri, B. Lee, and D. Niyato, "Robust cloud resource provisioning for cloud computing environments," in *Proc. IEEE SOCA*, Perth, WA, USA, 2010.
- [10] R. Kaewpuang, D. Niyato, P. Wang, and E. Hossain, "A framework for cooperative resource management in mobile cloud computing," *IEEE J. Sel. Areas Commun.*, vol. 31, no. 12, pp. 2685–2700, Dec. 2013.
- [11] Y. Li, J. Liu, B. Cao, and C. Wang, "Joint optimization of radio and virtual machine resources with uncertain user demands in mobile cloud computing," *IEEE Trans. Multimedia*, vol. 20, no. 9, pp. 2427–2438, Sept. 2018.
- [12] D. Bertsimas, E. Litvinov, X. A. Sun, J. Zhao, and T. Zheng, "Adaptive robust optimization for the security constrained unit commitment problem," *IEEE Trans. Power Syst.* vol. 28, no. 1, pp. 52–63, Feb. 2013.
- [13] B. Zeng and L. Zhao, "Solving two-stage robust optimization problems using a column-and-constraint generation method," *Operations Research L.*, pp. 457–461, vol. 41, no. 5, 2013.
- [14] V. Farhadi, F. Mehmeti, T. He, T.L. Porta, H. Khamfroush, S. Wang, K.S. Chan, "Service placement and request scheduling for data-intensive applications in edge clouds," in *IEEE INFOCOM*, Apr. 2019.
- [15] D.T. Nguyen, L.B. Le, and V.K. Bhargava, "Edge computing resource procurement: an online optimization approach," in *Proc. IEEE WF-IoT*, pp. 807–812, Singapore, 2018.
- [16] Z. Xu, W. Liang, W. Xu, M. Jia, and S. Guo, "Efficient algorithms for capacitated cloudlet placements," *IEEE Trans. Parallel Distrib. Syst.*, vol. 27, no. 10, pp. 2866–2880, Oct. 2016.
- [17] M. Jia, J. Cao, and W. Liang, "Optimal cloudlet placement and user to cloudlet allocation in wireless metropolitan area networks," *IEEE Trans. Cloud Comput.*, vol. 5, no. 4, pp. 725–737, Oct.–Dec. 2017.
- [18] L. Ma, J. Wu, and L. Chen, "DOTA: delay bounded optimal cloudlet deployment and user association in WMANs," in *Proc. IEEE/ACM CCGRID*, Madrid, Spain, 2017.
- [19] L. Wang, L. Jiao, T. He, J. Li, and M. Muhlhauser, "Service entity placement for social virtual reality applications in edge computing," in *Proc. IEEE INFOCOM*, Honolulu, HI, USA, 2018.
- [20] L. Zhao, W. Sun, Y. Shi, and J. Liu, "Optimal placement of cloudlets for access delay minimization in SDN-based internet of things networks," *IEEE Internet Things J.*, vol. 5, no. 2, pp. 1334–1344, April 2018.
- [21] S. Yang, F. Li, M. Shen, X. Chen, X. Fu, and Y. Wang, "Cloudlet placement and task allocation in mobile edge computing," *IEEE Internet Things J.*, vol. 6, no. 3, pp. 5853–5863, Jun. 2019.
- [22] A. Ceselli, M. Premoli and S. Secci, "Mobile edge cloud network design optimization," *IEEE/ACM Trans. Netw.*, vol. 25, no. 3, pp. 1818–1831, Jun. 2017.
- [23] S. Mondal, G. Das, and E. Wong, "CCOMPASSION: a hybrid cloudlet placement framework over passive optical access networks," in *Proc. IEEE INFOCOM*, Honolulu, HI, USA, 2018.
- [24] F. Haider, D. Zhang, M. St-Hilaire, and C. Makaya, "On the planning and design problem of fog computing networks," *IEEE Trans. Cloud Comput.*, to be published.
- [25] L. Yang, J. Cao, G. Liang, and X. Han, "Cost aware service placement and load dispatching in mobile cloud systems," *IEEE Trans. Comput.*, vol. 65, no. 5, pp. 1440–1452, May 2016.
- [26] D. Zeng, L. Gu, S. Guo, Z. Cheng, and S. Yu, "Joint optimization of task scheduling and image placement in fog computing supported software-defined embedded system," *IEEE Trans. Comput.*, vol. 65, no. 12, pp. 3702–3712, Dec. 2016.
- [27] R. Yu, G. Xue, and X. Zhang, "Provisioning QoS-aware and robust applications in internet of things: a network perspective," *IEEE/ACM Trans. Netw.*, vol. 27, no. 5, pp. 1931–1944, Oct. 2019.
- [28] S. Pasteris, S. Wang, M. Herbst, and T. He, "Service placement with provable guarantees in heterogeneous edge computing systems," in *Proc. IEEE INFOCOM*, Paris, France, Apr. 2019.
- [29] Q. Fan and N. Ansari, "Application aware workload allocation for edge computing-based IoT," *IEEE Internet Things J.*, vol. 5, no. 3, pp. 2146–2153, Jun. 2018.
- [30] A. Yousefpour et al., "FogPlan: a lightweight QoS-aware dynamic fog service provisioning framework," *IEEE Internet Things J.*, vol. 6, no. 3, pp. 5080–5096, Jun. 2019.
- [31] B. Gao, Z. Zhou, F. Liu, and F. Xu, "Winning at the starting line: joint network selection and service placement for mobile edge computing," in *Proc. IEEE INFOCOM*, pp. 1459–1467, Paris, France, 2019.
- [32] N. Kherraf, H.A. Alameddine, S. Sharafeddine, C. Assi, and A. Ghrayeb, "Optimized provisioning of edge computing resources with heterogeneous workload in IoT networks," *IEEE Trans. Netw. Serv. Manag.*, to be published.
- [33] K. Poularakis, J. Llorca, A. Tulino, I. Taylor, and L. Tassiulas, "Joint service placement and request routing in multi-cell mobile edge computing networks," in *Proc. IEEE INFOCOM*, Paris, France, Apr. 2019.
- [34] T. Ouyang, R. Li, X. Chen, Z. Zhou and X. Tang, "Adaptive user-managed service placement for mobile edge computing: an online learning approach," in *Proc. IEEE INFOCOM*, pp. 1468–1476, Paris, France, 2019.
- [35] L. Chen, J. Xu, S. Ren, and P. Zhou, "Spatio-temporal edge service placement: a bandit learning approach," *IEEE Trans. Wirel. Commun.*, vol. 17, no. 12, pp. 8388–8401, Dec. 2018.
- [36] B. Zeng and L. Zhao, "Electronic companion – Solving two-stage robust optimization problems using a column-and-constraint generation method," *Operations Research L.*, 2013.
- [37] Y. Mao, C. You, J. Zhang, K. Huang, and K. B. Letaief, "A survey on mobile edge computing: the communication perspective," *IEEE Commun. Surv. Tut.*, vol. 19, no. 4, pp. 2322–2358, Fourthquarter 2017.
- [38] H. Zhang, Y. Xiao, S. Bu, D. Niyato, F.R. Yu, and Z. Han, "Computing resource allocation in three-tier IoT fog networks: a joint optimization approach combining stackelberg game and matching," *IEEE Internet Things J.*, vol. 4, no. 5, pp. 1204–1215, Oct. 2017.
- [39] M. Jia, W. Liang, Z. Xu, M. Huang, and Y. Ma, "QoS-aware cloudlet load balancing in wireless metropolitan area networks," *IEEE Trans. Cloud Comput.*, to be published.
- [40] R. Deng, R. Lu, C. Lai, T.H. Luan, and H. Liang, "Optimal workload allocation in fog-cloud computing toward balanced delay and power consumption," *IEEE Internet Things J.*, vol. 3, no. 6, pp. 1171–1181, Dec. 2016.
- [41] R. Albert, H. Jeong, and A.L. Barabasi, "Internet: diameter of the world-wide web," *Nature*, vol. 401, no. 6749, pp. 130–131, 1999.
- [42] Z. Xu, W. Liang, A. Galis, Y. Ma, Q. Xia, and W. Xu, "Throughput optimization for admitting NFV-enabled requests in cloud networks," *Computer Networks*, vol. 143, pp. 15–29, 2018.
- [43] N. Kherraf, S. Sharafeddine, C. Assi, and A. Ghrayeb, "Latency and reliability-aware workload assignment in IoT networks with mobile edge clouds," *IEEE Trans. Netw. Ser. Manag.*, vol. 16, no. 4, pp. 1435–1449, Dec. 2019.
- [44] <https://aws.amazon.com/ec2/pricing/on-demand/>
- [45] S. Boyd and L. Vandenberghe, "Convex Optimization", Cambridge, U.K.: Cambridge Univ. Press, 2004.
- [46] J. Fortuny-Amat and B. McCarl, "A representation and economic interpretation of a two-level programming problem," *J. Oper. Res. Soc.*, vol. 32, no. 9, pp. 783–792, Sep. 1981.

APPENDIX

A. Deterministic Formulation

The deterministic formulation of the service placement and sizing problem is the following MILP problem:

$$\min_{x,y,z} \sum_j f_j(1 - z_j^0)z_j + \sum_j s_j z_j + p_0 y_0 + \sum_j p_j y_j + \beta \left\{ \sum_i d_{i,0} x_{i,0} + \sum_{i,j} d_{i,j} x_{i,j} \right\} \quad (58)$$

subject to

$$\sum_j z_j \geq r^{\min} \quad (59)$$

$$y_j \leq z_j C_j, \quad \forall j \quad (60)$$

$$\sum_j f_j(1 - z_j^0)z_j + \sum_j s_j z_j + p_0 y_0 + \sum_j p_j y_j \leq B \quad (61)$$

$$w \sum_i x_{i,0} \leq y_0 \quad (62)$$

$$w \sum_i x_{i,j} \leq y_j, \quad \forall j \quad (63)$$

$$x_{i,0} + \sum_j x_{i,j} = \lambda_i, \quad \forall i \quad (64)$$

$$d^{\text{avg}} = \frac{\sum_i d_{i,0}x_{i,0} + \sum_i \sum_j d_{i,j}x_{i,j}}{\sum_i \lambda_i^f} \quad (65)$$

$$d^{\text{avg}} \leq D^m \quad (66)$$

$$z_j \in \{0, 1\}; \quad y_0 \geq 0; \quad y_j \geq 0, \quad \forall j \quad (67)$$

$$x_{i,0} \geq 0, \quad \forall i; \quad x_{i,j} \geq 0, \quad \forall i, j. \quad (68)$$

In the deterministic algorithm in the simulation section, the SP first solves this deterministic problem, using the forecast demand λ^f , to obtain the optimal values of z and y (i.e., the amount of resource that the SP buy from the cloud and the ENs). Note that the SP can decide the optimal workload allocation (i.e., x) after observing the actual workload. However, the SP does not know the actual demand when making the resource procurement decision. Thus, the procured resources may not be able to serve the actual demand when the actual demand is much higher than the forecast value, which makes the workload allocation problem become infeasible.

Therefore, we define x_i^D as the number of requests at AP i that are unserved (i.e., dropped requests) in the operation stage. Let $x^D = \{x_1^D, x_2^D, \dots, x_M^D\}$. Also, denote by v^p the penalty for unserved requests. Let $Drop$ be the ratio between the total number of unserved requests and the total number of requests, i.e., $Drop = \frac{\sum_i x_i^D}{\sum_i \lambda_i}$, where λ_i is the actual workload arriving at AP i in the operation stage. Given the realization of demand $\lambda = \{\lambda_1, \lambda_2, \dots, \lambda_M\}$, the SP solves the following problem to determine the optimal workload allocation:

$$\min_{x, x^D} \beta \left\{ \sum_i d_{i,0}x_{i,0} + \sum_{i,j} d_{i,j}x_{i,j} \right\} + v^p \frac{\sum_i x_i^D}{\sum_i \lambda_i} \quad (69)$$

subject to

$$w \sum_i x_{i,0} \leq y_0 \quad (70)$$

$$w \sum_i x_{i,j} \leq y_j, \quad \forall j, \quad (71)$$

$$x_{i,0} + x_i^D + \sum_j x_{i,j} = \lambda_i, \quad \forall i, \quad (72)$$

$$\sum_i d_{i,0}x_{i,0} + \sum_{i,j} d_{i,j}x_{i,j} \leq D^m \sum_i \left(x_{i,0} + \sum_j x_{i,j} \right) \quad (73)$$

$$z_j \in \{0, 1\}; \quad y_0 \geq 0; \quad y_j \geq 0, \quad \forall j \quad (74)$$

$$x_{i,0}, x_i^D \geq 0, \quad \forall i; \quad x_{i,j} \geq 0, \quad \forall i, j, \quad (75)$$

where y is the optimal solution to the problem (58)-(68). Note that the maximum average delay constraint (73) is enforced for served requests only.

For the performance evaluation section in the paper, we compare the performance of the RO, ARO and the deterministic approaches. For example, similar to the procedures above, in the ARO approach, the SP first obtains the optimal value of y^{ARO} by solving the two-stage RO problem (22) and use it as input to the problem (69)-(75) to determine the optimal workload allocation decision with each realization of the actual workload. Note that for sufficiently large values of the penalty parameter v^p , the optimal x_i^D in this ARO approach is equal to zero for every i (i.e., no dropped requests) since y^{ARO} is robust against any demand realization in the uncertainty set.

B. Robust Optimization Formulation

In the static robust service placement and sizing problem, the placement, sizing, and workload allocation decisions are made simultaneously before knowing the actual demand. Based on the RO theory [8], the robust service placement and sizing problem can be expressed as follows:

$$\begin{aligned} \min_{(x,y,z) \in \mathcal{S}(x,y,z)} \quad & \max_{\lambda \in \mathcal{D}} \sum_j f_j(1 - z_j^0)z_j + \sum_j s_j z_j + p_0 y_0 \\ & + \sum_j p_j y_j + \beta \left\{ \sum_i d_{i,0}x_{i,0} + \sum_{i,j} d_{i,j}x_{i,j} \right\} \end{aligned} \quad (76)$$

subject to

$$x_{i,0} + \sum_j x_{i,j} \geq \lambda_i, \quad \forall i, \lambda \in \mathcal{D} \quad (77)$$

$$\sum_i d_{i,0}x_{i,0} + \sum_i \sum_j d_{i,j}x_{i,j} \leq D^m \sum_i \lambda_i, \lambda \in \mathcal{D}, \quad (78)$$

where

$$\mathcal{D}(\lambda^f, \hat{\lambda}, \Gamma) = \left\{ \begin{array}{l} \lambda_i = \lambda_i^f + g_i \hat{\lambda}_i, \quad \forall i; \quad g_i \in [-1, 1], \forall i \\ \sum_i |g_i| \leq \Gamma \end{array} \right\}, \quad (79)$$

$$\mathcal{S}(x,y,z) = \left\{ \begin{array}{l} \sum_j z_j \geq r^{\min}, \\ \sum_j h_j z_j + p_0 y_0 + \sum_j p_j y_j \leq B, \\ y_j \leq z_j C_j, \quad \forall j, \\ w \sum_i x_{i,j} \leq y_j, \quad \forall j, \\ w \sum_i x_{i,0} \leq y_0 \\ z_j \in \{0, 1\}; \quad y_0 \geq 0; \quad y_j \geq 0, \quad \forall j \\ x_{i,0} \geq 0, \quad \forall i; \quad x_{i,j} \geq 0, \quad \forall i, j \end{array} \right\} \quad (80)$$

Note that in the deterministic formulation, both equality and inequality constraints will produce the same result since equality happens at the optimality for cost minimization objective. Furthermore, equality constraint related to uncertainty is meaningless in the RO approach [8]. Thus, we write the workload balance constraints in form of inequality constraints as in (77).

Since the objective function (76) does not contain uncertainty parameters, we can alternatively write the robust problem as:

$$\min_{(x,y,z) \in \mathcal{S}(x,Y,Z)} \sum_j f_j(1 - z_j^0)z_j + \sum_j s_j z_j + p_0 y_0 + \sum_j p_j y_j + \beta \left\{ \sum_i d_{i,0} x_{i,0} + \sum_{i,j} d_{i,j} x_{i,j} \right\} \quad (81)$$

subject to

$$x_{i,0} + \sum_j x_{i,j} \geq \max_{\lambda \in \mathcal{D}} \lambda_i \quad (82)$$

$$\sum_i d_{i,0} x_{i,0} + \sum_{i,j} d_{i,j} x_{i,j} \leq D^m \min_{\lambda \in \mathcal{D}} \sum_i \lambda_i. \quad (83)$$

Consider constraint (83). First, observe that $\min_{\lambda \in \mathcal{D}} \sum_i \lambda_i$ can be expressed as:

$$\min_g \sum_i \left(\lambda_i^f + g_i \hat{\lambda}_i \right) \quad (84)$$

subject to

$$\sum_i |g_i| \leq \Gamma; \quad |g_i| \leq 1, \quad \forall i. \quad (85)$$

The problem (84)-(85) above is equivalent to:

$$\min_{g, t} \sum_i g_i \hat{\lambda}_i \quad (86)$$

subject to

$$\sum_i t_i \leq \Gamma, \quad (u) \quad (87)$$

$$-t_i + g_i \leq 0, \quad \forall i \quad (v_i) \quad (88)$$

$$-t_i - g_i \leq 0, \quad \forall i \quad (\gamma_i) \quad (89)$$

$$g_i \leq 1, \quad \forall i \quad (\mu_i) \quad (90)$$

$$-g_i \leq 1, \quad \forall i \quad (\sigma_i) \quad (91)$$

where $u, v, \gamma, \mu, \sigma$ are the dual variables associated with the constraints. This is a linear program. Based on duality in linear programming, the dual linear program of this problem is:

$$\max_{u,v,\gamma,\mu,\sigma} -u\Gamma - \sum_i \mu_i - \sum_i \sigma_i \quad (92)$$

subject to

$$v_i - \gamma_i + \mu_i - \sigma_i \leq -\hat{\lambda}_i, \quad \forall i \quad (93)$$

$$u - v_i - \gamma_i \geq 0, \quad \forall i \quad (94)$$

$$u \geq 0; \quad v_i \geq 0, \quad \gamma_i \geq 0, \quad \mu_i \geq 0, \quad \sigma_i \geq 0, \forall i. \quad (95)$$

Additionally, we have:

$$x_{i,0} + \sum_j x_{i,j} \geq \max_{\lambda \in \mathcal{D}} \lambda_i = \max_{\lambda \in \mathcal{D}} \left(\lambda_i^f + g_i \hat{\lambda}_i \right). \quad (96)$$

In the set \mathcal{D} , we have $\sum_i 1 \cdot |g_i| \leq \Gamma$ and $-1 \leq g_i \leq 1$. Hence, $\max_{\lambda \in \mathcal{D}} g_i = \min \left\{ 1, \frac{\Gamma}{1} \right\}$. Consequently, (96) is equivalent to:

$$x_{i,0} + \sum_j x_{i,j} \geq \lambda_i^f + \min \left\{ 1, \Gamma \right\} \hat{\lambda}_i. \quad (97)$$

Finally, the static (single-stage) robust service placement and workload allocation problem can be written as follows:

$$\min_{(x,y,z) \in \mathcal{S}(x,Y,Z)} \sum_j f_j(1 - z_j^0)z_j + \sum_j s_j z_j + p_0 y_0 + \sum_j p_j y_j + \beta \left\{ \sum_i d_{i,0} x_{i,0} + \sum_{i,j} d_{i,j} x_{i,j} \right\} \quad (98)$$

subject to

$$x_{i,0} + \sum_j x_{i,j} \geq \lambda_i^f + \min \left\{ 1, \Gamma \right\} \hat{\lambda}_i \quad (99)$$

$$\sum_i d_{i,0} x_{i,0} + \sum_{i,j} d_{i,j} x_{i,j} \quad (100)$$

$$\leq D^m \sum_i \lambda_i^f - D^m \left(u\Gamma + \sum_i \mu_i + \sum_i \sigma_i \right)$$

$$u\Gamma + \sum_i \mu_i + \sum_i \sigma_i = - \sum_i g_i \hat{\lambda}_i \quad (101)$$

$$\sum_i t_i \leq \Gamma \quad (102)$$

$$-t_i + g_i \leq 0, \quad \forall i \quad (103)$$

$$-t_i - g_i \leq 0, \quad \forall i \quad (104)$$

$$g_i \leq 1, \quad \forall i \quad (105)$$

$$-g_i \leq 1, \quad \forall i \quad (106)$$

$$v_i - \gamma_i + \mu_i - \sigma_i \leq -\hat{\lambda}_i, \quad \forall i \quad (107)$$

$$u - v_i - \gamma_i \geq 0, \quad \forall i \quad (108)$$

$$u \geq 0; \quad v_i \geq 0; \quad \gamma_i \geq 0; \quad \mu_i \geq 0; \quad \sigma_i \geq 0, \forall i. \quad (109)$$

This is an MILP problem, which can be efficiently solved using solvers such as Gurobi. Note that the maximum operator in the average delay constraint (100) is removed because at the optimum (i.e., minimum) of the robust problem (98)-(109), the last term in the right hand side of (100) should be maximized so that the feasibility set is largest.

C. The KKT Conditions

The Lagrangian function of the inner minimization problem (38)-(44) in the subproblem **SP** is:

$$\begin{aligned} \mathcal{L}(x, \pi_0, \pi_j, \mu, \sigma_i, \xi_{i,0}, \xi_{i,j}) = & - \sum_{i,j} \xi_{i,j} x_{i,j} - \sum_i x_{i,0} \xi_{i,0} \\ & + \beta \left(\sum_i d_{i,0} x_{i,0} + \sum_{i,j} d_{i,j} x_{i,j} \right) + \pi_0 (w \sum_i x_{i,0} - y_0) \\ & + \sum_j \pi_j (w \sum_i x_{i,j} - y_j) + \sum_i \sigma_i (\lambda_i - x_{i,0} - \sum_j x_{i,j}) \\ & + \mu \left(\sum_i d_{i,0} x_{i,0} + \sum_{i,j} d_{i,j} x_{i,j} - D^m \sum_i \lambda_i \right) \end{aligned}$$

The KKT conditions give

$$\frac{\partial \mathcal{L}}{\partial x_{i,0}} = \beta d_{i,0} + w\pi_0 + \mu d_{i,0} - \sigma_i - \xi_{i,0} = 0, \quad \forall i \quad (110)$$

$$\frac{\partial \mathcal{L}}{\partial x_{i,j}} = \beta d_{i,j} + w\pi_j + \mu d_{i,j} - \sigma_i - \xi_{i,j} = 0, \quad \forall i, j \quad (111)$$

$$w \sum_i x_{i,0} \leq y_0; \quad w \sum_i x_{i,j} \leq y_j, \quad \forall j \quad (112)$$

$$\sum_i d_{i,0} x_{i,0} + \sum_{i,j} d_{i,j} x_{i,j} \leq D^m \sum_i \lambda_i, \quad (113)$$

$$x_{i,0} + \sum_j x_{i,j} = \lambda_i, \forall i; x_{i,0} \geq 0, \forall i; x_{i,j} \geq 0, \forall i, j \quad (114)$$

$$\pi_0 \geq 0; \pi_j \geq 0, \forall j; \mu \geq 0; \sigma_i \geq 0, \forall i \quad (115)$$

$$\xi_{i,0} \geq 0, \forall i; \xi_{i,j} \geq 0, \forall i, j \quad (116)$$

$$(y_0 - w \sum_i x_{i,0})\pi_0 = 0; (y_j - w \sum_i x_{i,j})\pi_j = 0, \forall j \quad (117)$$

$$(D^m \sum_i \lambda_i - \sum_i d_{i,0}x_{i,0} - \sum_{i,j} d_{i,j}x_{i,j})\mu = 0 \quad (118)$$

$$x_{i,0}\xi_{i,0} = 0, \forall i; x_{i,j}\xi_{i,j} = 0, \forall i, j, \quad (119)$$

where (110)-(111) are the stationary conditions, (112)-(114) are the primal feasibility conditions, (115)-(116) are the dual feasibility conditions, and (117)-(119) are complementary slackness conditions. From (110)-(111), we have:

$$\beta d_{i,0} + w\pi_0 + \mu d_{i,0} - \sigma_i = \xi_{i,0} \geq 0, \forall i \quad (120)$$

$$\beta d_{i,j} + w\pi_j + \mu d_{i,j} - \sigma_i = \xi_{i,j} \geq 0, \forall i, j \quad (121)$$

From (119), if $x_{i,0} \geq 0$, then $\xi_{i,0} = 0$ and $\beta d_{i,0} + w\pi_0 + \mu d_{i,0} - \sigma_i = 0$. Thus, $(\beta d_{i,0} + w\pi_0 + \mu d_{i,0} - \sigma_i)x_{i,0} = 0, \forall i$. Similarly, we have $(\beta d_{i,j} + w\pi_j + \mu d_{i,j} - \sigma_i)x_{i,j} = 0, \forall i, j$. On the other hand, assume $(\beta d_{i,0} + w\pi_0 + \mu d_{i,0} - \sigma_i)x_{i,0} = 0, \forall i$. If $x_{i,0} > 0$, then $\beta d_{i,0} + w\pi_0 + \mu d_{i,0} - \sigma_i = 0$, which implies $\xi_{i,0} = 0$. Hence, $x_{i,0}\xi_{i,0} = 0, \forall i$. Similarly, $(\beta d_{i,j} + w\pi_j + \mu d_{i,j} - \sigma_i)x_{i,j} = 0, \forall i, j$ implies $x_{i,j}\xi_{i,j} = 0, \forall i, j$.

Therefore, it is easy to see that the KKT conditions (110)-(119) and the set of constraints (46)-(50) are equivalent. It is worth noting that we can directly use the set of KKT conditions (110)-(119) to solve the subproblem, but it will involve more variables (i.e., ξ_0 and ξ) compared to solving the subproblem with (46)-(50). Furthermore, the set of constraints (46)-(50) can be informally and quickly obtained by using duality in linear programming, without explicitly writing down the Lagrangian and KKT conditions.

D. The Complete MILP Formulation for the Subproblem

By applying the Fortuny-Amat transformation [46] to every complimentary constraint in the problem (45)-(53), we obtain the equivalent MILP (37) as follows:

$$\max_{x, \lambda, \pi_0, \pi_j, \mu, \sigma_i, u} \beta \left\{ \sum_i d_{i,0}x_{i,0} + \sum_{i,j} d_{i,j}x_{i,j} \right\} \quad (122)$$

subject to

$$0 \leq \beta d_{i,0} + w\pi_0 + \mu d_{i,0} - \sigma_i \leq u_i^0 M_i^0, \forall i \quad (123)$$

$$0 \leq x_{i,0} \leq (1 - u_i^0) M_i^0, \forall i \quad (124)$$

$$0 \leq \beta d_{i,j} + w\pi_j + \mu d_{i,j} - \sigma_i \leq u_{i,j}^1 M_{i,j}^1, \forall i, j \quad (125)$$

$$0 \leq x_{i,j} \leq (1 - u_{i,j}^1) M_{i,j}^1, \forall i, j \quad (126)$$

$$0 \leq y_0 - w \sum_i x_{i,0} \leq u^2 M^2 \quad (127)$$

$$0 \leq \pi_0 \leq (1 - u^2) M^2 \quad (128)$$

$$0 \leq y_j - w \sum_i x_{i,j} \leq u_j^3 M_j^3, \forall j \quad (129)$$

$$0 \leq \pi_j \leq (1 - u_j^3) M_j^3, \forall j \quad (130)$$

$$0 \leq D^m \sum_i \lambda_i - \sum_i d_{i,0}x_{i,0} - \sum_{i,j} d_{i,j}x_{i,j} \leq u^4 M^4 \quad (131)$$

$$0 \leq \mu \leq (1 - u^4) M^4 \quad (132)$$

$$u_i^0 \in \{0, 1\}, \forall i; u_{i,j}^1 \in \{0, 1\}, \forall i, j \quad (133)$$

$$u^2, u^4 \in \{0, 1\}; u_j^3 \in \{0, 1\} \quad (134)$$

$$x_{i,0} + \sum_j x_{i,j} = \lambda_i, \forall i \quad (135)$$

$$\lambda_i = \lambda_i^f + g_i \hat{\lambda}_i, \forall i; \sum_i t_i \leq \Gamma; t_i \leq 1, \forall i \quad (136)$$

$$-t_i + g_i \leq 0, \forall i; t_i + g_i \geq 0, \forall i, \quad (137)$$

where u represents the set of binary variables u^0, u^1, u^2, u^3, u^4 . Also, $M_i^0, M_{i,j}^1, M^2, M_j^3, M^4, M_i^5$ are sufficiently large numbers. The value of each M should be large enough to ensure feasibility of the associated constraint. On the other hand, the value of each M should not be too large to enhance the computational speed of the solver. Indeed, the value of each M should be tighten to the limits of parameters and variables in the corresponding constraint. For instance, M_i^0 needs to be larger or equal to the maximum value of $x_{i,0}$, which is λ_i . Thus, M_i^0 can be set to be a small number greater than λ_i .

Additionally, it is easy to see that, for the maximization problem (122)–(137), g_i should be nonnegative for every i to maximize the objective function (see constraints (131), (135), (136), (137)). Hence, we can simplify (136)-(137) as

$$\lambda_i = \lambda_i^f + t_i \hat{\lambda}_i, \forall i; \sum_i t_i \leq \Gamma; 0 \leq t_i \leq 1, \forall i. \quad (138)$$

E. Convergence of Algorithm 1

Algorithm 1 converges to the optimal value of the original two-stage robust problem (22) in $O(K)$ iterations. Indeed, this can be shown by contradiction that any repeated λ^* implies $LB = UB$. Specifically, assume (z^*, y^*, η^*) is the optimal solution to MP (57), (λ^*, x^*) is the optimal solution to the SP in iteration k , and λ^* appears in a previous iteration. From step 4 of **Algorithm 1**, we have: $UB \leq \sum_j h_j z_j^* + \sum_j p_j y_j^* + p_0 y_0^* + \beta \left(\sum_i d_{i,0} x_{i,0}^* + \sum_{i,j} d_{i,j} x_{i,j}^* \right) = RHS$. Now, since λ^* appears in a previous iteration, the MP in iteration $k+1$ is identical to the MP in iteration k . Hence, (z^*, y^*, η^*) is also the optimal solution to the MP in iteration $k+1$. We have: $LB \geq \sum_j h_j z_j^* + \sum_j p_j y_j^* + p_0 y_0^* + \eta^*$. Since the extreme scenario λ^* has already been identified and related constraints are added to the MP before iteration k , we have: $\eta^* \geq \beta \left(\sum_i d_{i,0} x_{i,0}^* + \sum_{i,j} d_{i,j} x_{i,j}^* \right)$. Thus,

$LB \geq RHS \geq UB$, which implies $LB = UB$. As a result, **Algorithm 1** converges in a finite number of iterations. Typically, the algorithm converges within a few iterations as shown in the numerical results.

F. Stochastic Formulation

The stochastic formulation of the service placement and sizing problem is the following MILP problem:

$$\min_{x,y,z} \sum_j f_j(1-z_j^0)z_j + \sum_j s_j z_j + p_0 y_0 + \sum_j p_j y_j + \sum_{\xi} \eta^{\xi} \left\{ \beta \left(\sum_i d_{i,0} x_{i,0}^{\xi} + \sum_{i,j} d_{i,j} x_{i,j}^{\xi} \right) \right\} \quad (139)$$

subject to

$$\sum_j z_j \geq r^{\min} \quad (140)$$

$$y_j \leq z_j C_j, \quad \forall j \quad (141)$$

$$\sum_j f_j(1-z_j^0)z_j + \sum_j s_j z_j + p_0 y_0 + \sum_j p_j y_j \leq B \quad (142)$$

$$w \sum_i x_{i,0}^{\xi} \leq y_0; \quad w \sum_i x_{i,j}^{\xi} \leq y_j, \quad \forall j, \xi \quad (143)$$

$$x_{i,0}^{\xi} + \sum_j x_{i,j}^{\xi} = \lambda_i^{\xi}, \quad \forall i, \xi \quad (144)$$

$$\sum_i d_{i,0} x_{i,0}^{\xi} + \sum_{i,j} d_{i,j} x_{i,j}^{\xi} \leq \sum_i \lambda_i^w D^m, \quad \forall \xi \quad (145)$$

$$z_j \in \{0, 1\}; \quad y_0 \geq 0; \quad y_j \geq 0, \quad \forall j \quad (146)$$

$$x_{i,0}^{\xi} \geq 0, \quad \forall i; \quad x_{i,j}^{\xi} \geq 0, \quad \forall i, j, \xi. \quad (147)$$

Note that ξ is the scenario index and η^{ξ} is the probability of scenario ξ , where λ_i^{ξ} is the demand at AP i in scenario ξ . Also, $x_{i,j}^{\xi}$ is the workload allocated from AP i to EN j and $x_{i,0}^{\xi}$ is the workload allocated from AP i to the cloud in scenario ξ . The meaning of the variables and constraints in the stochastic model is similar to those in the deterministic model in *Appendix A*. The main difference is that we consider a set of scenarios in the stochastic model to express the uncertainty.

The stochastic model assumes that η^{ξ} and the demand at every AP in each scenario ξ are known and given as input to the problem (139)–(147). Thus, the stochastic approach needs to know the exact probability distribution of the uncertainties to have a good performance. This information is hard to obtain in practice. Furthermore, the uncertainty realization may not follow the historical pattern (i.e., future can be different from the past). The proposed robust methods do not need the probability distribution information. Furthermore, the objective of a stochastic model is to optimize the “average” or “expected” system performance over all the scenarios, while

In the stochastic model (139)–(147), similar to the ARO model, the service placement and sizing decisions are made in the first stage before the uncertainty is revealed. Given the first-stage decisions, the workload allocation decision is

the goal of a robust model is to optimize the “worst-case” performance. Thus, the design objectives of the stochastic and robust approaches are different. The optimal solution obtained from a stochastic model can perform badly in worse-case scenarios, especially for long-tail distributions.

determined in the second stage after knowing the actual demand realization. Since the actual demand can be different from the generated scenarios (which can be understood as training scenarios), we need to evaluate the performance of the stochastic model in the actual operation stage over a set of testing scenarios. As in the deterministic model, the procured resources in the first-stage of the stochastic model may not be sufficient to serve the actual demand and the SP may need to drop some requests.

To compare the performance of the stochastic approach with the deterministic and robust approaches, we generate 1000 training demand scenarios to represent the demand uncertainty. The scenario set is then used as the input to the stochastic problem (139)–(147) to determine the optimal placement and sizing solution in the first stage. Then, similar to Section V-B2 in the main manuscript, we generate 100 testing demand scenarios to compare the performance of different schemes.

Fig. 12 illustrate the performance of the deterministic, stochastic (SO), RO, ARO approaches. To evaluate the performance of the stochastic approach, we need to assume that we know the exact distribution of the demand across different areas to generate a set of training demand scenarios. Since the exact distribution is hard to obtain and also future data can be different from the historical pattern, the actual performance of the stochastic model can be worse than the reported performance in Fig. 12 where we assume to know the exact probability distribution of the demand. For the results in Fig. 12, the demand distribution at the APs is assumed to follow a multivariate normal distribution. We have also run simulations with other distributions and obtained similar trends and observations on the performance comparison of the four approaches. The SO solution outperforms the deterministic one since it captures the uncertainty, but it is still much worse than the proposed robust models.

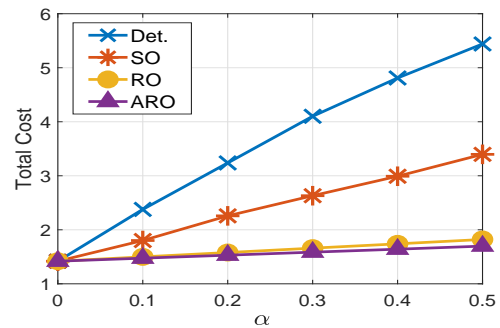


Fig. 12: Worst-case cost comparison in the operation stage